European Journal of Geography

The publication of the European Journal of Geography (EJG) is based on the European Association of Geographers' goal to make European Geography a worldwide reference and standard. Thus, the scope of the EJG is to publish original and innovative papers that will substantially improve, in a theoretical, conceptual, or empirical way the quality of research, learning, teaching, and applying geography, as well as in promoting the significance of geography as a discipline. Submissions are encouraged to have a European dimension. The European Journal of Geography is a peer-reviewed open access journal and is published quarterly.

Research Article

Understanding Dynamics of Land Use & Land Cover Change Using GIS & Change Detection Techniques in Tartous, Syria

Ali Younes[1,2*], **Adnan Ahmad**[3], **Ashok D. Hanjagi**[1] **& Archana M. Nair**[3]

[1] Department of Geography, Bangalore University, India
[2] Department of Geography, University of Tartous, Syria
[3] Department of Civil Engineering, Indian Institute of Technology Guwahati, India
* Correspondence: ali.h.you1994@gmail.com

Abstract: Although Tartous governorate accounts for only 1% of the total land area of Syria, it recorded the highest burden of Internally Displaced Persons (IDPs) during the Syrian crisis, with nearly half a million IDPs seeking refuge there in 2014. The simultaneous population growth and economic recession exacerbated the exploitation of natural resources and led to environmental degradation. The study aims to understand the dynamics of land use and land cover change (LULCC) in Tartous from 1987 to 2019 by comparing two periods, be-fore and during the crisis, through the integration of remote sensing and GIS using the change detection-based post-classification comparison technique. The results showed significant LULCC that revealed significant changes during the crisis compared to before. However, most of the changes have negative environ-mental impacts, especially near built-up areas and in the northeast, where natural vegetation decreased by 40% by 2019, of which about 60% is due to agricultural expansion. Conversely, built-up areas have doubled, from 18 km2 in 1987 to 34 km2 in 2019, mainly at the expense of agricultural land. Meanwhile, agricultural land remained the predominant land use, with almost 74% of the study area reflecting primary economic activity. Nevertheless, a particular expansion was recorded during the crisis compared to before. The study highlights the impact of anthropogenic pressures on the environment, especially during wars. The findings provide important insights for policymakers and researchers concerned with sustainable land management and environmental conservation in war-affected regions. It also recommends developing comprehensive, multi-level plans to address the complex challenges in similar contexts.

Keywords: LULCC Dynamics, Change Detection, Environmental Impact, Remote Sensing, GIS, Sustainable Land Management, Environmental Conservation, Syria, IDPs, wars.

Received: 18/04/2023
Revised: 30/06/2023
Accepted: 08/07/2023
Published: 13/07/2023

DOI: 10.48088/ejg.a.you.14.3.020.041

Highlights:

- Tartous recorded the highest burden of IDPs in 2014, with more than half a million.
- The Post-Classification Comparison (PCC) technique is a powerful tool for monitoring the dynamics of LULCC.
- Significant LULCC was observed, with notable fluctuations during the crisis compared to before.
- Most of the LULCC had negative environmental impacts, especially in the western and northeastern regions.
- The growing population and economic recession in Syria put pressure on land resources and affect the environment in the search for livelihoods.

1. Introduction

Land evolves and changes over time. Today's urban areas most likely developed from agricultural land, and today's plantations were probably forests in the past. Land is a precious but scarce resource with limited potential to be restored after the change (Rahaman et al., 2020), and human use affects over 70% of the global ice-free land area (IPCC, 2019). Therefore, the ever-increasing population and economic globalisation are forcing the acquisition of more and more land and accelerating competition in land use (Halder, 2018; Lambin & Meyfroidt, 2011). It has been projected that future urbanisation trends could lead to an almost threefold increase in global urban land area between 2000 and 2030 (United Nations, 2019), increasing pressure on land resources (Seto et al., 2012; Vishwakarma et al., 2016). Land use refers to the various aspects of human use of land, including agricultural land, built-up areas, pastures, etc. In contrast, land cover includes the biotic and abiotic elements on the earth's surface, such as natural vegetation, water bodies, wetlands, etc. (Pandian et al., 2014).

Land Use and Land Cover Change (LULCC) can be triggered by natural and anthropogenic drivers, the latter consisting of proximate and underly-ing causes (Lambin et al., 2001). The proximate causes of LULCC are human activities, including slow factors such as demographic changes and rapid factors such as conflict and socio-economic shocks (Aide & Grau, 2004; Lambin & Meyfroidt, 2011; Rudel et al., 2005). The proximate caus-es can directly alter local LULC and potentially lead to structural changes in socio-ecological systems. On the other hand, the underlying causes of LULCC are socio-economic, biophysical, cultural and technological factors that operate at national, regional and global scales. These factors in-teract in complex ways and across spatial and temporal patterns. It is important to note that these factors are not isolated but interconnected (Geist & Lambin, 2002; Lambin & Meyfroidt, 2011; Wilson & Wilson, 2013).

LULCC significantly impacts microclimate by altering the energy exchange between land and atmosphere (Parveen et al., 2018). It also contrib-utes to global climate change by altering the amount of greenhouse gases in the atmosphere, leading to changes in temperature and precipitation patterns. In addition, deforestation, urbanisation and agricultural expansion are examples of LULCC practices that can increase carbon dioxide (CO2) emissions and contribute to global warming (IPCC, 2019; Santos et al., 2021). Therefore, monitoring LULCC is essential for operational planning, governance and management of land resources (Lam, 2008), land surface temperature control (Kafy et al., 2020; Mohamed, 2021b), mitigation of soil erosion (Abdo, 2018; Alsafadi et al., 2022; Mohammed et al., 2020) and natural hazards (Abdo, 2020; Li & Deng, 2017), conservation of natural habitats (Mohamed et al., 2020) and biodiversity (Butt et al., 2015).

Change detection is crucial for managing and monitoring natural resources and urban development (Hassan et al., 2016). It is widely used to determine and describe changes in LULC properties using multitemporal remote sensing data (Attri et al., 2015). The main objective of change detection is to analyse the historical impact of an event quantitatively. It provides a detailed record of spatial distribution as well as qualitative and quantitative information on feature changes (Butt et al., 2015; El-Hattab, 2016). A competent change detection application must provide details on the changed area, rate and spatial extent of the changed LULC (Attri et al., 2015; Butt et al., 2015). Several techniques have already been developed and applied for change detection in LULC studies. However, post-classification comparison (PCC) is the most accurate approach in this area (Butt et al., 2015; Hassan et al., 2016). PCC involves comparing independent classifications from different points in time by presenting detailed LULCC (from-to) data (Morgan & Hodgson, 2021). It captures the extent and direction of spatial changes in LULC. Comparable thematic classes are created for each classification, and changes can be visualised using a change matrix that indicates the number of pixels in each class for both time points (Attri et al., 2015; Morgan & Hodgson, 2021).

Remote Sensing (RS) and Geographic Information Systems (GIS) have proved to be valuable tools for understanding the global, physical processes that shape the earth (Mallupattu & Sreenivasula Reddy, 2013). They are considered robust for observing, monitoring, assessing and mapping LULCC dynamics due to their accuracy, digital format and repeated data collection (Chaikaew, 2019; Hassan et al., 2016; Twisa & Buchroithner, 2019). Advances in RS technology and associated digital image processing have enabled the integration of larger volumes of geographic data with GIS (Mallupattu & Sreenivasula Reddy, 2013), providing unprecedented opportunities to detect LULCC more accurately over larger areas, with reduced costs and processing times (Attri et al., 2015). RS and GIS are widely used to assist decision-makers in planning, development and conservation by presenting multiple alternatives to protect the environment (Khandve & Mokadam, 2011; Omusotsi, 2019). It also provides useful information for many applications in sustainable land management, environmental conservation and socio-economic change (Abeed et al., 2021; Kulo, 2018).

Many studies on LULC in war-affected areas attempt to understand the dynamics of LULCC under war conditions. However, it is important to note that the impact of war on LULC is complex and varies depending on the local context (Eklund et al., 2017). They can have simultaneous positive and negative impacts on the environment, such as forest regrowth and restoration (Landholm et al., 2019). Undoubtedly, wars have significant impacts on LULC, not only through direct changes in LULC dynamics, abandonment of agricultural land and forest fires but also indirectly, e.g., through forced migration and displacement of local people (Cazabat, 2018). According to Cazabat (2018), the most important impact of human displacement is the overexploitation of natural resources caused by the loss of forest land and water resources. For example, the impact of the Colombian conflict on LULCC in the Andean-Amazonian region was studied by Murillo-Sandoval et al. (2021) from 1988 to 2019. It showed that land cover did not change significantly during the conflict (1988-2011), but in the post-conflict period (2012-2019), 40% more forests were converted to agricultural land. Similarly, Landholm et al. (2019) pointed out that the Colombian conflict had mostly negative impacts on forests. In conflict-affected areas, forests were eight times more likely to be deforested in subsequent years than the average deforestation rate. Eklund et al. (2017) found that land grabbing by the Islamic State (IS) in Syria and Iraq since 2014 has led to changes in agriculture, including expansion of cropland into previously uncultivated areas, abandonment of cropland and a decline in high-intensity cropland. Abeed et al. (2021) also concluded that the rise of ISIS in northeastern Syria led to a shift in cropping patterns and forced landowners to manage their land. Heidarlou et al. (2020) studied the impact of the Iraq-Iran war on land use and forest cover changes in Zagros forests in Iran over 22 years. They found that forest cover was converted to different land uses, such as cropland and built-up areas, with the greatest decline occurring before and after the war. The onset of the war led to less conversion of forests as people were resettled in safer areas, reducing anthropogenic pressure on forest resources.

LULC in Syria is constantly changing due to many factors, including growing population, climate change, economic development and ecosystem change (Abdo, 2018; Mohamed, 2021a; Mohamed et al., 2020; Rahmoun et al., 2018) and in the last decade mainly due to war and its aftermath, which has led to significant displacement of people from the country and also within the country, moving from the interior towards coastal areas in search of safer living conditions (Hammad et al., 2018). Müller et al. (2016) studied the impact of Syrian refugees on LULC and freshwater resources. They found that due to the war and subsequent migration, irrigated agricultural land in Syria and storage of winter precipitation in Syrian dams decreased by about 50%. Similarly, Al-Husban & Ayen (2020) studied the impact of the Syrian war on LULC in Al-Yarmouk basin in southern Syria and found that irrigated areas decreased by 12% over eight years while cultivated areas increased by 1.7%. Jaafar et al. (2015) also found a decline in irrigated agricultural production in the Orontes Basin from 15% to 30% between 2000 and 2013. Mohamed (2021b) studied LULCC in Syria's two largest cities, Damascus and Aleppo. It was reported that from 2010 to 2018, there was a decrease in agricultural land and green areas and an increase in bare land. In addition, built-up areas have decreased in Aleppo, while there has been an in-crease in Damascus.

The coastal region of Syria, which includes the governorates of Tartous and Lattakia, was comparatively less affected during the crisis than other regions, making it a viable refuge for inland residents (Mohamed et al., 2020). Some studies examined the LULCC in the coastal region and pro-vided a valuable record of regional LULC characteristics. Abdo (2018) investigated the impact of the war in Syria on vegetation and found that forest cover, most likely dense forest cover, declined over the last 30 years in the southern Syrian coastal region. Several factors are responsible for this deterioration. First, inefficiencies in forest protection and management result in too many trees being cut down for fuel wood (Hammad et al., 2018; Mohamed, 2021a). Second, the increase in agricultural production and the expansion of agricultural land due to the growing population (Abdo, 2018; Rahmoun et al., 2018). Third, climate change, global warming and frequent forest fires (Mohamed, 2021a; Mohamed et al., 2020). In addition, it has been noted that the growing population has led to a significant expansion of urban areas at the expense of forest and agricultural land (Hammad et al., 2018; Mohamed, 2021a; Rahmoun et al., 2018).

Since March 2011, i.e., the outbreak of the Syrian war, Tartous governorate, which forms the southern part of the coastal region, has witnessed a massive influx of IDPs who fled to Tartous in search of safety (Abdo, 2018; Faour & Fayad, 2014). Tartous governorate covers 1% of Syria's total land area. Over the years, the population of Tartous increased from 663,000 in 1990 to 797000 in 2011, representing 4% of the total population (OCHA, 2014; Rahmoun et al., 2018). In October 2014, the number of IDPs in Tartous governorate was estimated at 452,000, of which 53%

were in Tartous sub-district, i.e., the study area (OCHA, 2014). Although the number of IDPs in Tartous is lower than in other governorates, the burden of IDPs in Tartous was the highest at 47% (Doocy et al., 2015). As a result, this displacement led to overexploitation of land resources, resulting in landscape changes, land degradation, degradation of water resources, loss of natural vegetation and urban sprawl (Dudley et al., 2002; Rudel et al., 2005), which ultimately affected the dynamics of the LULC in Tartous (Faour & Fayad, 2014; Mohamed et al., 2020).

Based on the findings described in the literature and the context of Tartous governorate before and during the Syrian crisis, the study aims to understand the LULCC dynamics in Tartous from 1987 to 2019 by integrating the techniques of RS and GIS. The objectives are summarised as follows:

- to monitor LULCC dynamics in Tartous before (1987-2005) and during the Syrian crisis (2013-2019).
- to track the direction and extent of LULC transformations.
- to examine the spatial changes in natural vegetation cover, agricultural land and built-up areas.
- to understand the environmental impacts of these changes.
- to highlight the spatio-temporal extent of built-up areas.

The study aims to enrich international geographical research by deepening the understanding of LULCC dynamics and its potential environmental impacts. It provides a basis for future research and progress in this field. Furthermore, it can contribute to sustainable land management and environmental conservation in the war-affected regions in Syria and beyond.

2. Materials and Methods

2.1. Study Area

The sub-district of Tartous (hereafter Tartous) is located in the coastal region of Syria and has a total area of 197 km2. It is located between lati-tudes 34°46'35" N - 34°57'59" N and longitudes 35°51'46" E - 36°03'40" E and forms the westernmost part of Tartous governorate (Figure 1), which includes Tartous City, the largest and central city in the governorate, and the second largest port in Syria (Rahmoun et al., 2018). The area belongs to the humid and sub-humid climates of Syria (Zakhem & Hafez, 2010), with a significant influence of the Mediterranean Sea, which brings heavy rainfall of more than 800 mm per year from October to May, while the hot and dry summer lasts from June to September. The average annual temperature is 20°C (Faour & Fayad, 2014). The study area comprises two distinct zones in terms of relief, the coastal plain characterised by fertile soils in the west and the gradually rising hills with lower-quality soils in the east (Ibrahim et al., 2014) (Figure 1). The latter is characterised by a traditional terrace cropping system for growing tree crops on the slopes. This system increases grain yields, prevents soil erosion, maintains soil fertility, and ensures consistent long-term production (Jain & Singh, 2003).

The study area has different socio-economic characteristics, with an urban centre and a hinterland with an agricultural character. It is known for its lush and fertile Mediterranean agriculture, including irrigated and rain-fed systems (Ibrahim et al., 2014; Jain & Singh, 2003) and contributes significantly to national agricultural production (OCHA, 2014). Olive and citrus trees, wheat and vegetables are the main crops grown in the region, in addition to greenhouse farming, which is widespread in the southern part (Mohamed, 2021a). Therefore, the predominant LULC in the study area is agricultural land with scattered natural vegetation along the hilltops and riparian zones, i.e., the strip of land between the channels of the rivers and the mountain slopes (McGlynn & Seibert, 2003). The built-up areas include Tartous City, the primary urban centre on the coast, and numerous towns and villages scattered throughout the study area.

2.2. Data Acquisition

The selection of appropriate satellite images is essential for successfully implementing LULC monitoring and mapping. The images must have adequate spatial and temporal resolution to produce highly accurate and relevant maps and estimates (Pickering et al., 2021). In studies focusing on historical LULCC dynamics, Landsat satellites are considered the most appropriate data source because of their extensive archive of images dating back to the 1980s (Mohamed, 2021b; Pickering et al., 2021).

Six images were acquired from three different satellite datasets, covering the period from 1987 to 2019 (Table 1 and Figure 2). They were obtained free of charge from the official United States Geological Survey (USGS) portal. The selection of the other two satellite datasets, i.e. Sentinel-2B and Terra/Aster, for the years 2005 and 2019, respectively, was due to the unavailability of data according to the following fact-based criteria: (i) The study area is characterised by its coastal location, with prevailing westerly, southerly and southwesterly winds blowing from the Mediterranean Sea throughout the year (Zakhem & Hafez, 2010), resulting in persistent cloud cover. As a result, obtaining cloud-free images is a major challenge. Therefore, an exhaustive search was conducted to ensure that the selected images are cloud-free, thus minimising the impact of atmospheric attenuation and water vapour content on LULC classification. (ii) The optimal monitoring period for LULC is during the growing season due to photosynthetic activity (Tucker et al., 2004). In Syria, this period corresponds to the spring season, which usually starts in March and lasts until June (Zakhem & Hafez, 2010). The spring season is characterised by increased vegetation growth after the wet winter (Al-Fares, 2013). Therefore, all selected images were taken based on these two criteria.

In addition, two scenes of the Shuttle Radar Topography Mission (SRTM) with a spatial resolution of 30 m (1 arc-second) (USGS, 2023b) were downloaded free of charge from the official USGS portal and mosaicked to create a digital elevation model (DEM) of the study area (Figure 1).

The integration of additional data as external inputs in LULC monitoring studies is a well-established and documented practise in remote sensing (Lu & Weng, 2007; Mohamed, 2021a). As it was not possible to conduct field observations in the study area, various additional data sources were used to meet all objectives coherently. These sources included high-resolution Google Earth archive data, topographic maps and an assessment study by the International Centre for Agricultural Research in Dry Areas (ICARDA) (De Pauw et al., 2004). In addition, previous studies on LULC in the Syrian coastal region were consulted to identify the predominant LULC classes and their distribution in the study area (Faour & Fayad, 2014; Hammad et al., 2018; Mohamed, 2021a; Rahmoun et al., 2018). Therefore, including the external data sources compensated for the lack of ground truth data.

https://doi.org/10.48088/ejg.a.you.14.3.020.041

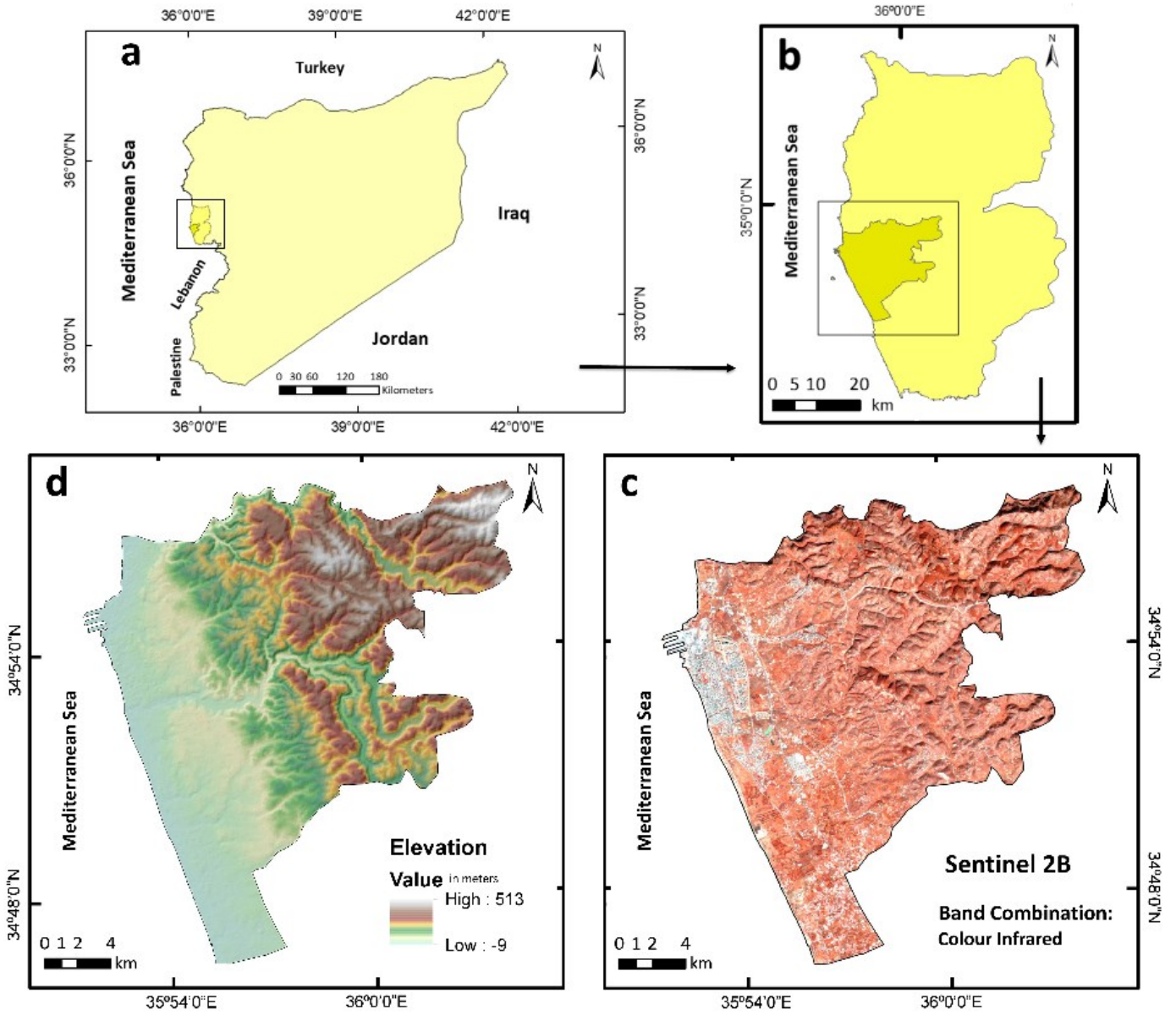

Figure 1. Location of the study area: Syrian Arab Republic (a), Tartous Governorate (b), Tartous Sub-district (c) and (d), Satellite image of the study area in CIR band combination in 2019 (c), DEM map showing elevation of the study area (d).

Table 1. Characteristics of the satellite images used in the study.

No.	Year	Satellite	Sensor	Resolution	Swath Width	CIR Band Combination (Infrared, Red, Green)
1.	1987	Landsat 5	Multispectral Scanner (MSS)	60m[1]	185 km	3, 2, 1
2.	1992	Landsat 5	Thematic Mapper (TM)	30m	183 km	4, 3, 2
3.	1999					
4.	2005	Terra	Advanced Spaceborne Thermal Emission and Reflection Radiometer (ASTER)	15m[2]	60 km	3N, 2, 1
5.	2013	Landsat 8	Operational Land Imager (OLI)	30m	183 km	5, 4, 3
6.	2019	Sentinel-2B	Multispectral Imager (MSI)	10m[3]	290 km	8, 4, 3

[1,2,3] *Resampled to 30m*

2.3. Data Processing and Classification

Before classification, the visible and near-infrared spectral bands were combined to produce the required multispectral images for analysis. The study area was fully covered in a single scene in all three satellite datasets, eliminating the need for mosaicking. Each image was clipped to match the extent of the study area. The swath width for each sensor is listed in Table 1 (ESA, 2023; NASA, 2023a; USGS, 2023c). The colour infrared band combination (CIR) was used as the standard false colour composite to facilitate visual interpretation and differentiation of LULC (USGS, 2023a). CIR is obtained by combining near-infrared, red and green bands (Table 1). This combination of bands facilitates the detection of vegetation in the images based on their spectral reflectance properties (EOS, 2023), with vegetation appearing in different shades of red. Soil is ob-served in different shades of brown, while urban areas are characterised by cyan-blue or yellow/grey tones, depending on their composition. While clear water is shown in dark bluish tones, turbid water appears cyan due to the reflection of the sediment (NASA, 2023b) (Figure 1).

Since change detection methods do not support images with different spatial resolutions, a possible and common technique to overcome this problem is to perform spatial resampling by manipulating the high-resolution data to match the lower resolution of the other dataset or vice versa, i.e., upscaling or downscaling, thereby unifying the spatial resolutions (Ferraris et al., 2017; Park et al., 2019). For this reason, three images, namely Landsat 5 MSS (1987), ASTER (2005) and Sentinel-2B (2019), were resampled to a uniform spatial resolution of 30 metres before being used for change detection analysis. Nearest Neighbour Resampling is a technique commonly used in remote sensing. It involves assigning a value to each resampled pixel based on the nearest corresponding pixel in the original image. Although this method is simple, fast and preserves the original pixel values, it can result in some loss of detail (Park et al., 2019; Porwal & Katiyar, 2014). To compensate for this loss, we performed an accuracy assessment to verify the satisfactory accuracy of the LULC classification. We also compared our results with those published in the literature. To achieve the objectives of the study, three image processing and GIS platforms were used, namely ERDAS Imagine 2014, QGIS 3.28.3 and ArcMap 10.4. The flowchart of the methodology is shown in Figure 2.

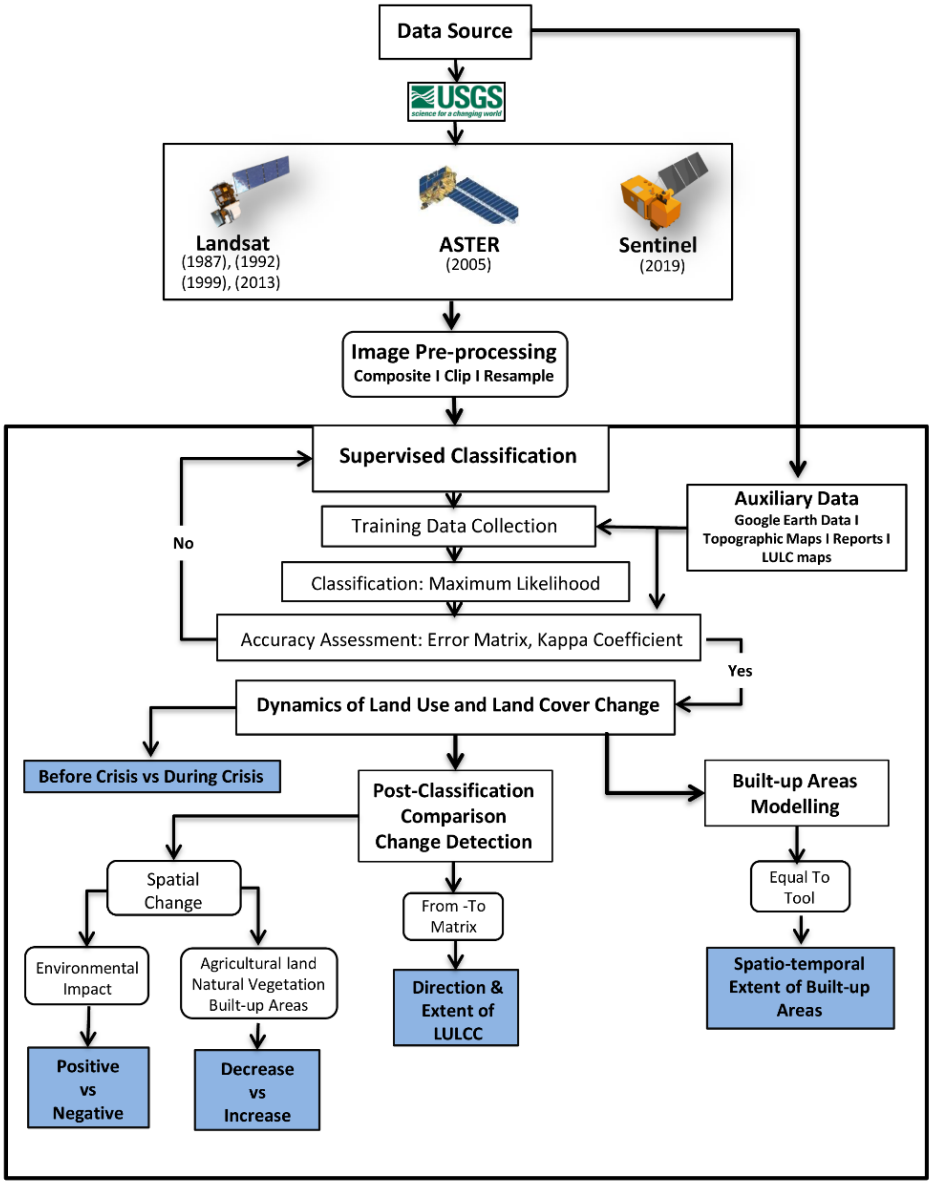

Figure 2. Methodology flowchart.

https://doi.org/10.48088/ejg.a.you.14.3.020.041

The supervised method is one of two automatic methods for classifying satellite images. It was used for the classification process of the study due to its accuracy compared to the unsupervised method and the fact that the analyst has complete control over the classes by selecting the representative pixels, thus providing more reliable results (Abburu & Babu Golla, 2015; Enderle & Weih Jr., 2005; Twisa & Buchroithner, 2019). Maximum Likelihood Classification (MLC) is a supervised classification algorithm that assigns pixels to the appropriate classes based on the probability values of the pixels. This study used MLC because it is more advantageous and easier to adopt for non-complex terrains with well-defined LULC categories. Moreover, it is a robust algorithm with high accuracy that hardly leads to misclassification (Abburu & Babu Golla, 2015; Chakraborty et al., 2017; Sisodia et al., 2014). Processing MLC requires at least 10 to 30 independent training signatures per class to accurately assess the mean and variance to produce representative descriptions of the relevant classes (Foody & Mathur, 2004). However, the number can be increased if a class has significant variability (Schowengerdt, 2007). It is recommended that these training signatures are well representative, numerous and span the study area to capture all levels of natural variance in spectral response (Chen & Stow, 2002; Foody & Mathur, 2004). Prior knowledge of the study area and external supplementary data were considered to locate at least 20 training sites per LULC class. The LULC classes studied are water bodies, barren land, fallow land, agricultural land, natural vegetation and built-up areas Table 2.

Table 2. LULC classes used in the study and their corresponding description.

Class	Description
Water bodies	onshore zone of the Mediterranean and freshwater bodies (streams, ponds, swamps, etc.)
Barren Land	beaches, exposed rock, uncultivable exposed soil, and transitional areas (agricultural land to built-up areas)
Natural Vegetation	forest (broad-leaved forests, natural coniferous forests), shrublands, and bushes.
Agricultural Land	cropland, orchards, horticultural land, greenhouses, and farmlands not cultivated for less than one year.
Fallow Land	farmlands not cultivated for more than one year, and transitional areas (natural vegetation to agricultural land).
Built-up Areas	residential, commercial, services, industrial areas, transportation and utilities.

2.4. Accuracy Assessment

Accuracy assessment is crucial for the verification and validation of classification results. It is performed to compare the classified map with reference data (Chaikaew, 2019; Mohajane et al., 2018; Mosammam et al., 2017), which may be a trusted data source or ground truth (ESRI, 2023a). Collecting ground truth data in the field can be resource-intensive and time-consuming. Alternatively, ground truth data can be obtained by interpreting high-resolution images, existing classified data or GIS data layers (ESRI, 2023a).

In our study, reference data were based on the following reliable sources: (i) prior knowledge of the study area, (ii) validation and comparison with high-resolution images, i.e. Google Earth data of the nearest date, (iii) comparable classified maps of the study area (Mohamed, 2021a; Rahmoun et al., 2018), (iv) 1:50000 scale topographic maps. We created a confusion matrix and calculated the overall accuracy (OA), user accuracy (UA) and producer accuracy (PA) of classification results to assess potential errors in the classification process (Congalton & Green, 2019). A widely used method for assessing the accuracy of classified maps is to generate a series of random points from the reference data (ESRI, 2023a). This is done using the stratified random method, where the number of points in each class corresponds to its relative area. In general, the number of points depends on several factors, such as the size of the study area, the number of classes and the objective of the mapping, although a number of at least fifty points is recommended (Anand, 2012). However, according to Finegold & Ortmann (2016), the minimum number of points required is 20 to 100. Due to the small size of the study area, we relied on 75 validation points tested for each classified map to assess accuracy. We assessed these points by cross-referencing them with the reference data mentioned above.

In addition, the kappa coefficient was included in the accuracy assessment process. It is a statistical measure of association commonly used to assess the degree of agreement or precision in classification (Kraemer, 2015; Rwanga & Ndambuki, 2017). It serves as a quantitative indicator of the quality of a measure considering all elements of the error matrix and is defined in terms of errors (Anand, 2012; Kraemer, 2015; Talukdar et al., 2020). Kappa is calculated by comparing the proportion of observed agreement with the proportion of agreement expected by chance. The following formula can be used to calculate the kappa coefficient:

$$K^{\wedge} = (p_o - p_c) / (1 - p_c) \quad (1)$$

Where p_o is the proportion of units that agree, and p_c is the proportion of units for the expected chance agreement (Anand, 2012; Rwanga & Ndambuki, 2017). McHugh (2012) and Talukdar et al. (2020) have suggested that kappa results can be interpreted as follows: Values lower than 0.40 indicate poor agreement, values between 0.40 and 0.55 indicate fair agreement, values between 0.55 and 0.70 indicate good agreement, values between 0.70 and 0.85 indicate very good agreement, and values higher than 0.85 indicate excellent agreement. For detailed calculations, see (Anand, 2012; Kraemer, 2015; McHugh, 2012; Rwanga & Ndambuki, 2017; Talukdar et al., 2020).

2.5. Change Detection

Post-Classification Comparison (PCC), a change detection technique, was performed to achieve the following objectives (Figure 2):

- to track the direction and extent of LULC transformations. Accordingly, a two-way cross matrix was constructed to determine the quantitative transformations from one particular LULC class to another and the corresponding area on a pixel-to-pixel basis.
- to examine the spatial patterns of change in agricultural land, natural vegetation and built-up areas. Three categories were created: (i) In-crease, (ii) No Change and (iii) Decrease. Conversion of the LULC class in question to another LULC class is considered a decrease. In contrast, the conversion of another LULC to the class in question represents an increase.

- to understand the impact of the LULCC on the environment, considering five categories, (i) Positive Impact, (ii) Moderate Positive Impact, (iii) No Change, (iv) Moderate Negative Impact and (v) Negative Impact. Changes in spatial characteristics from land use to land cover were considered positive impacts on the environment; conversely, changes from land cover to land use were considered negative. However, spatial changes, such as the conversion of fallow land to agricultural land, were considered moderate positive. Spatial changes, such as the conversion of natural vegetation to agricultural land, were considered moderate negative (Chazdon et al., 2020; Fang et al., 2022; Hao & Ren, 2009; Hu et al., 2023; Krishnan & Firoz, 2021; Li & Deng, 2017; Pauleit et al., 2005; Rahaman et al., 2020; Sharma et al., 2023; Winowiecki et al., 2015).

2.6. Built-up Areas Modelling

To highlight the spatio-temporal extent of built-up areas, the Equal To tool was used in ArcMap GIS. This tool helps to select features within a layer that meet a certain attribute value or condition (ESRI, 2023b). It can help analyse or visualise spatial data based on certain criteria, such as LULC. It extracted the pixel values of built-up areas from each LULC map by performing a relational equal-to process for two inputs on a cell-by-cell basis (ESRI, 2023c). This technique provided six maps representing the spatio-temporal extent of the built-up areas during the study period.

3. Results

3.1. LULCC Dynamics

3.1.1. Before the Syrian Crisis (1987 to 2005)

During the first period, from 1987 to 2005 (hereafter before the Syrian crisis), the classification results show that the study area experienced significant changes in LULC (Figure 3 and Table 3). In 1987, agricultural land occupied the largest part of the study area with 74.8%, followed by natural vegetation with 10.2% and built-up areas with 9%. Fallow land and barren land had a smaller share of 3.1% and 2.1%, respectively; water bodies accounted for only 0.8%. However, high rates of change occurred by 2005, mainly with a decreasing trend, except for fallow land and built-up areas.

In 2005, agricultural land was still the largest LULC in the study area (Figure 3 and Table 3). However, their share decreased slightly compared to 1987. At the same time, the built-up areas increased by 47.5%. Natural vegetation decreased drastically by 31.5% compared to 1987. Barren land and water bodies decreased significantly by 56.1% and 43.8%, respectively. Fallow land, on the other hand, recorded an increase of 16.1% compared to 1987.

By examining LULCC dynamics in the study area before the Syrian crisis, it was found that agricultural land was consistently the largest LULC class, with a gradual decreasing trend over time. At the same time, natural vegetation decreased rapidly. Built-up areas increased continuously during all observations. Although fallow land showed a gradual increase from 1987 to 1999, this was followed by an abrupt decrease in 2005. Meanwhile, barren land and water bodies decreased steadily over time.

Table *3*. Area of LULC from 1987 to 2019 and the rate of change before and during the crisis.

	Year	Water bodies		Barren Land		Natural Vegetation		Agricultural Land		Fallow Land		Built-up Areas	
		Area		Area		Area		Area		Area		Area	
		km²	%	km²	%	km²	%	km²	%	km²	%	km²	%
Before Crisis	**1987**	1.6	0.8	4.1	2.1	20.3	10.2	149.3	74.8	6.2	3.1	18.1	9
	1992	1.0	0.5	2.4	1.2	19.5	9.8	148.2	74.8	8.4	4.2	18.7	9.4
	1999	0.9	0.4	2.8	1.4	15.8	8.0	143.6	72.5	13.6	6.9	21.4	10.8
	2005	0.9	0.4	1.8	0.9	13.9	7.0	146.3	74.4	7.2	3.6	26.7	13.6
	Change Rate (1987 – 2005)	**-43.8%**		**-56.1%**		**-31.5%**		**-2.0%**		**+16.1%**		**+47.5%**	
During Crisis	**2013**	1.0	0.5	2.8	1.4	12.9	6.5	148.6	74.9	3.9	2.0	29	14.6
	2019	0.4	0.2	0.8	0.4	12.3	6.3	149.1	75.6	0.8	0.4	33.8	17.1
	Change Rate (2013 – 2019)	**-60.0%**		**-71.4%**		**-4.7%**		**+0.3%**		**-79.5%**		**+16.6%**	

https://doi.org/10.48088/ejg.a.you.14.3.020.041

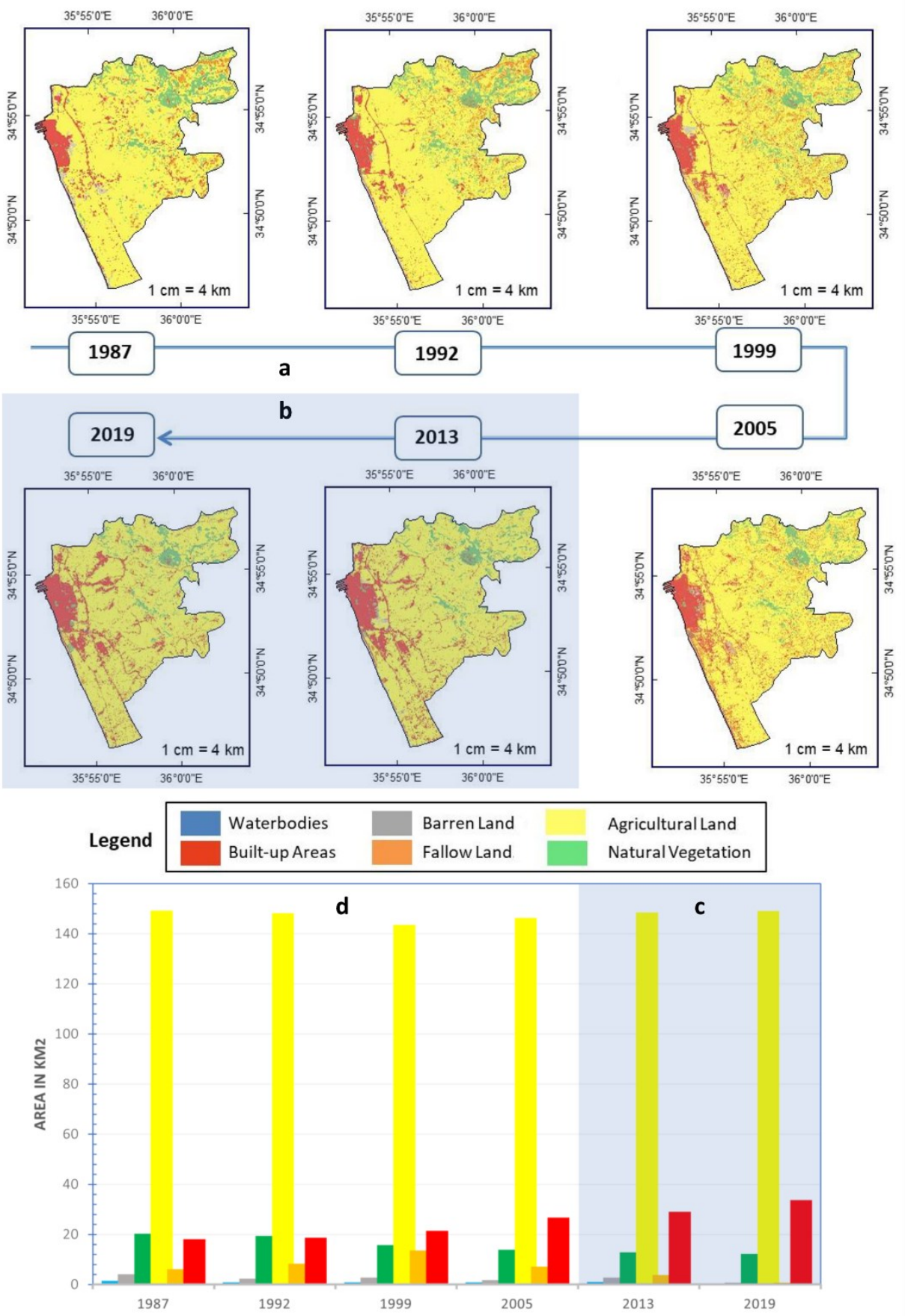

Figure 3. LULC distribution in the study area from 1987 to 2019, including before the crisis (a and d) and during the crisis (b and c)

https://doi.org/10.48088/ejg.a.you.14.3.020.041

3.1.2. During the Syrian Crisis (2013 to 2019)

During the second period, between 2013 and 2019 (hereafter during the Syrian crisis), significant changes in LULC continued to occur in the study area (Figure 3 and Table 3). In 2019, agricultural land was still the predominant class at 75.6% of the study area, with a slight increase of 0.3% compared to 2013. Built-up areas also continued to increase, with an increase of 17.1%. In contrast, natural vegetation decreased continuously by about 4.7%. Fallow and barren land recorded a significant decrease of 79.5% and 71.4%, respectively. The water bodies decreased by 60% compared to 2013.

Notable changes were observed in LULCC during the interval period, i.e., between 2005 and 2013. Most LULCs showed an increasing trend, except for natural vegetation and fallow land. Agricultural land increased by 1.6% in 2013 compared to 2005. Water bodies and barren land also increased unusually, by 11.1% and 55.6%, respectively. Built-up areas grew steadily by 10.8%. On the other hand, natural vegetation decreased by 7.2%, while fallow land abruptly decreased by 45.8%.

3.1.3. LULC Comparison Before and During the Syrian Crisis

Comparative analysis of LULCC dynamics over 18 years before the crisis and 6 years during the crisis has revealed notable differences between the two periods. Although agricultural land remained the predominant LULC class in both periods, it showed an increasing trend during the Syrian crisis, with a growth rate of 0.3% compared to before. Natural vegetation, on the other hand, showed a decreasing trend in both periods. Built-up areas recorded significant growth at a relatively constant rate during both periods. Barren land and water bodies showed a declining trend in both periods, with a higher rate during the crisis of 71.4% and 60%, respectively, compared to 56.1% and 43.8% before the crisis. Conversely, fallow land showed an increasing trend of 16.1% before the crisis and a significant decrease of 79.5% during the crisis (Figure 3 and Table 3).

3.2. Accuracy Assessment

Table 4 shows the error matrix, which includes the overall accuracy (OA), producer accuracy (PA), user accuracy (UA), and the kappa coefficient. The overall accuracy of the six LULC maps of 1987, 1992, 1999, 2005, 2013 and 2019 were 84%, 85.33%, 84%, 81.33%, 92% and 90.67%, respectively. The corresponding kappa values for the same years were 0.75, 0.78, 0.76, 0.73, 0.89 and 0.87, respectively. Based on the interpretation of the kappa results proposed by McHugh (2012) and Talukdar et al. (2020), the kappa values obtained show satisfactory classification accuracy.

3.3. LULC Change Detection

3.3.1. LULC transformations

The study used the PCC technique to determine LULC transformations from 1987 to 2019 (Figure 2). The results are presented in a cross-tabulation (Table 4), thematic map and chord diagram (Figure 4). It can be observed that 82.8% of agricultural land in 1987 has remained unchanged in 2019, while 13.3% has been converted to built-up areas and 3.2% has reverted to natural vegetation. 34.9% of the natural vegetation experienced no change between 1987 and 2019. Meanwhile, 60.4% was lost to agricultural land, and 4.3% was conversed into built-up areas.

Water bodies have retained only 21.3% of their total area between 1987 and 2019, while the rest has been replaced by barren land (24.7%), built-up areas (32.9%) and agricultural land (20.1%). Furthermore, 84.3% of the fallow land in 1987 was converted to agricultural land in 2019, and 13.2% was lost to built-up areas. Meanwhile, only 2.3% of the barren land in 1987 remained barren in 2019, while 42.6% was converted to built-up areas, 51.4% became agricultural land, and 2.8% changed into natural vegetation.

Table 4. Cross-tabulation matrix of LULC transformations between 1987 and 2019.

		2019											
	LULC Classes	**WB**		**BL**		**FL**		**AL**		**NV**		**BuA**	
		km²	**%**	**km²**	**%**	**km²**	**%**	**km²**	**%**	**km²**	**%**	**km²**	**%**
1987	**WB**	0.2	21.3	0.2	24.7	0.0	0.3	0.2	20.1	0.0	0.7	0.3	32.9
	BL	0.0	0.1	0.1	2.3	0.0	0.9	2.1	51.4	0.1	2.8	1.7	42.6
	FL	0.0	0.0	0.0	0.1	0.1	1.3	5.2	84.3	0.1	1.1	0.8	13.2
	AL	0.1	0.1	0.4	0.3	0.6	0.4	122.6	82.8	4.8	3.2	19.7	13.3
	NV	0.0	0.2	0.0	0.0	0.1	0.2	12.1	60.4	7.0	34.9	0.9	4.3
	BuA	0.0	0.2	0.1	0.5	0.1	0.4	6.9	38.7	0.4	2.3	10.4	58.0

https://doi.org/10.48088/ejg.a.you.14.3.020.041

Table 5. Cross-tabulation error matrix of classified vs reference data.

1987								
Classified Data	Reference Data							
	WB	BL	AL	BA	FL	NV	Total	UA
WB	4	0	0	0	0	0	4	100
BL	0	4	0	0	1	0	5	80
AL	0	0	38	0	1	3	42	90.5
BA	0	3	2	5	0	0	10	50
FL	0	0	0	0	4	1	5	80
NV	0	0	1	0	0	8	9	88.9
Total	4	7	41	5	6	12	75	
PA	100	57.1	92.7	100	66.7	66.7		
Overall Accuracy (OA) 84.00%				Kappa Coefficient 0.75				
1992								
Classified Data	Reference Data							
	WB	BL	AL	BA	FL	NV	Total	UA
WB	4	0	0	0	0	0	4	100
BL	0	6	0	0	0	0	6	100
AL	0	0	36	1	0	1	38	94.7
BA	0	0	3	6	1	0	10	60
FL	0	0	2	0	5	1	8	62.5
NV	0	0	2	0	0	7	9	77.8
Total	4	6	43	7	6	9	75	
PA	100	100	83.7	85.7	83.3	77.8		
Overall Accuracy (OA) 85.33%				Kappa Coefficient 0.78				
1999								
Classified Data	Reference Data							
	WB	BL	AL	BA	FL	NV	Total	UA
WB	4	0	0	0	0	0	4	100
BL	0	5	1	0	0	0	6	83.3
AL	0	1	35	0	0	2	38	92.1
BA	0	2	1	7	0	0	10	70
FL	0	0	3	0	5	0	8	62.5
NV	0	0	2	0	0	7	9	77.8
Total	4	8	42	7	5	9	75	
PA	100	62.5	83.3	100	100	77.8		
Overall Accuracy (OA) 84.00%				Kappa Coefficient 0.76				
2005								
Classified Data	Reference Data							
	WB	BL	AL	BA	FL	NV	Total	UA
WB	4	0	0	0	0	0	4	100
BL	0	3	0	3	0	0	A6	50
AL	0	2	33	0	0	3	38	86.8
BA	0	1	2	7	0	0	10	70
FL	0	1	1	1	5	0	8	62.5
NV	0	0	0	0	0	9	9	100
Total	4	7	36	11	5	12	75	
PA	100	42.9	91.7	63.6	100	75		
Overall Accuracy (OA) 81.33%				Kappa Coefficient 0.73				
2013								
Classified Data	Reference Data							
	WB	BL	AL	BA	FL	NV	Total	UA
WB	4	0	0	0	0	0	4	100
BL	0	5	0	1	0	0	6	83.3
AL	0	0	36	0	0	2	38	94.7
BA	0	1	0	9	0	0	10	90
FL	0	1	1	0	6	0	8	75
NV	0	0	0	0	0	9	9	100
Total	4	7	37	10	6	11	75	
PA	100	71.4	97.3	90	100	81.8		
Overall Accuracy (OA) 92.00%				Kappa Coefficient 0.89				
2019								
Classified Data	Reference Data							
	WB	BL	AL	BA	FL	NV	Total	UA
WB	4	0	0	0	0	0	4	100
BL	0	6	0	0	0	0	6	100
AL	0	0	36	0	0	2	38	94.7
BA	0	1	1	8	0	0	10	80
FL	0	1	0	2	5	0	8	62.5
NV	0	0	0	0	0	9	9	100
Total	4	8	37	10	5	11	75	
PA	100	75	97.3	80	100	81.8		
Overall Accuracy (OA) 90.67%				Kappa Coefficient 0.87				

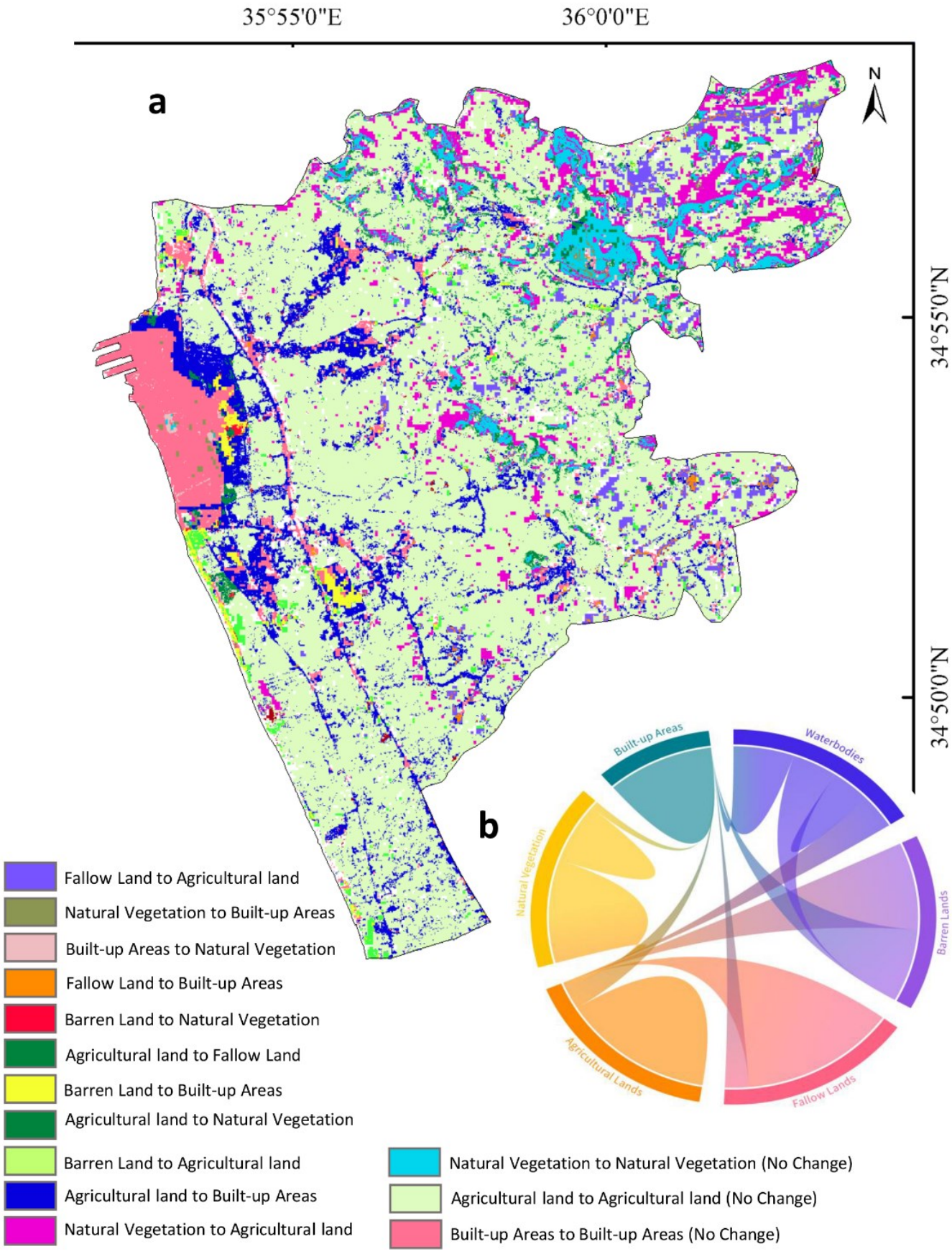

Figure 4. Distribution (**a**) and direction (**b**) of LULC transformations in the study area from 1987 to 2019.

https://doi.org/10.48088/ejg.a.you.14.3.020.041

3.3.2. Change Detection of Agricultural land

The study examined spatial changes in agricultural land, natural vegetation and built-up areas from 1987 to 2019. The results were classified into three categories: (i) Increase, (ii) No change, and (iii) Decrease. A significant spatial change occurred in agricultural land throughout the study period (Figure 5). There was a decrease near built-up areas in the west, indicating a conversion of agricultural land to built-up areas. Conversely, there was an increase in the hilly region in the northeast, indicating conversion of fallow land and natural vegetation to agricultural land.

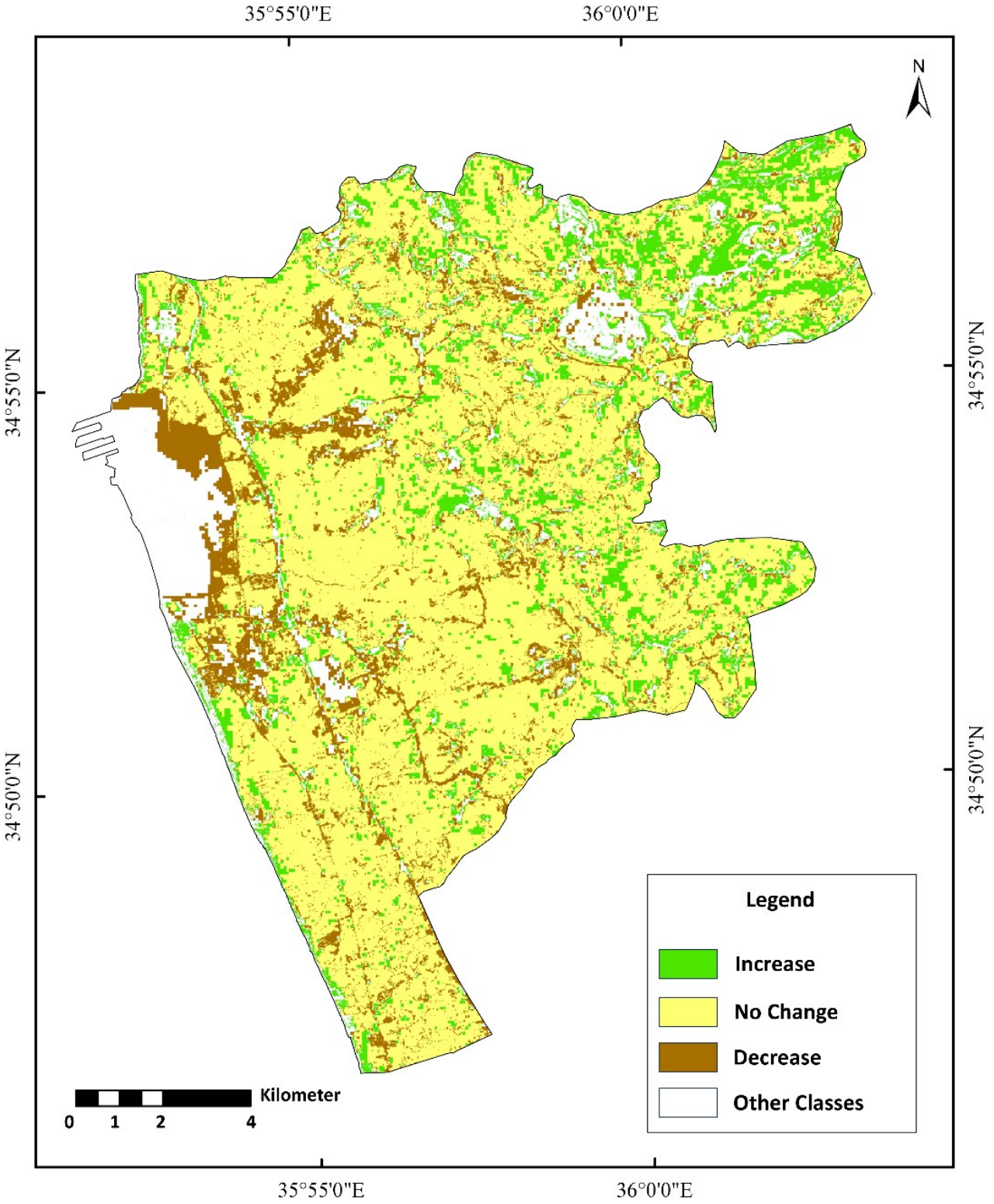

Figure 5. Agricultural land change from 1987 to 2019

https://doi.org/10.48088/ejg.a.you.14.3.020.041

3.3.3. Change Detection of Natural Vegetation

Analysis of changes in natural vegetation showed an obvious decline between 1987 and 2019, particularly in the hilly northeast of the study area (Figure 6. Natural vegetation change from 1987 to 2019). This decline is likely due to deforestation in favour of fallow land and agricultural land. However, the analysis also found a slight increase in scattered patches, possibly due to the regeneration of natural vegetation on previously abandoned land and the establishment of urban green spaces in Tartus City.

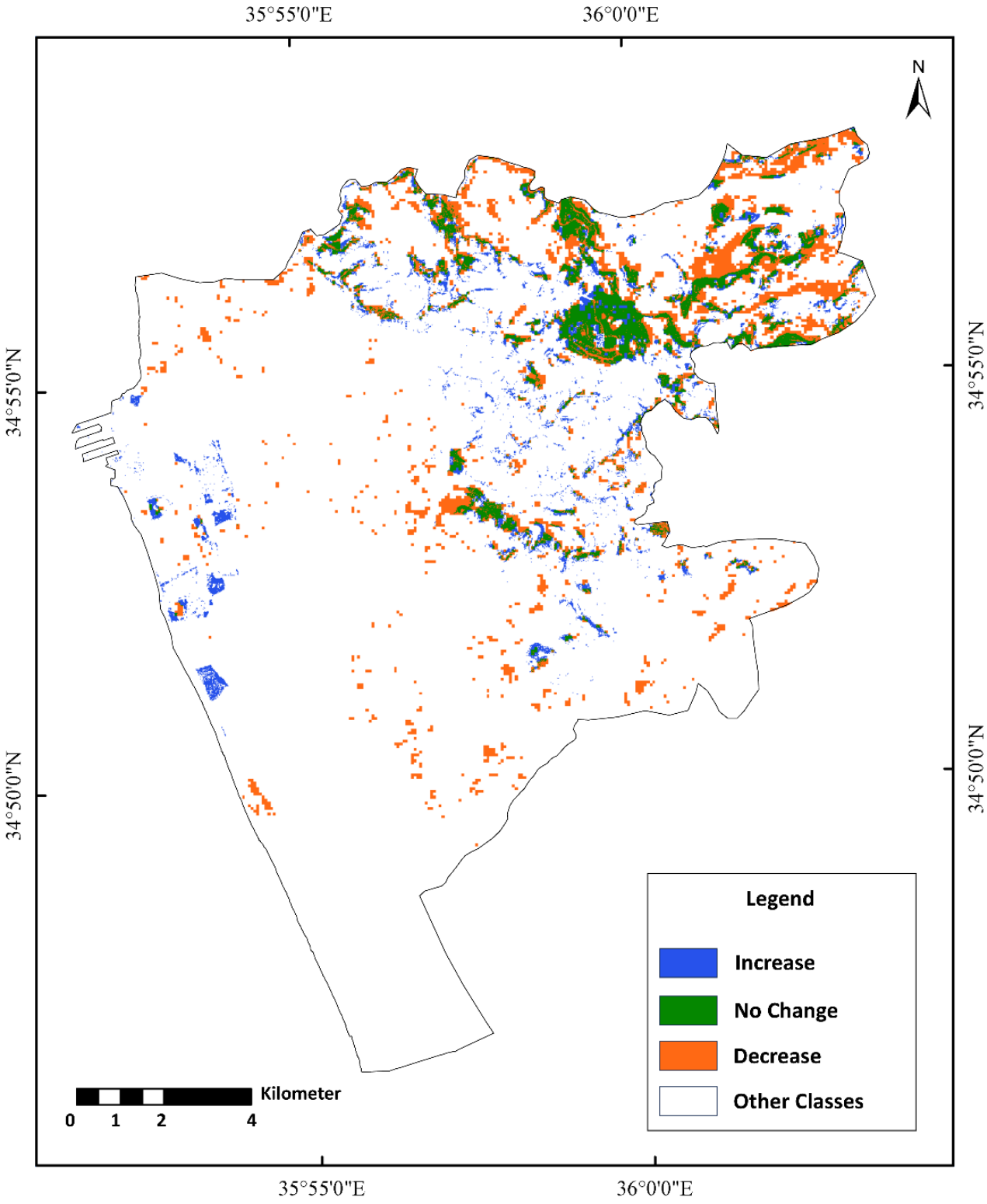

Figure 6. Natural vegetation change from 1987 to 2019.

https://doi.org/10.48088/ejg.a.you.14.3.020.041

3.3.4. Change Detection of Built-up Areas

The analysis showed significant growth in built-up areas between 1987 and 2019 (Figure 7). The spatial expansion was observed around pre-existing urban aggregates such as Tartous City and nearby towns and villages. It was suggested that pre-existing urban areas expanded steadily over the 32-year study period to develop larger urban aggregates in response to population growth in the study area.

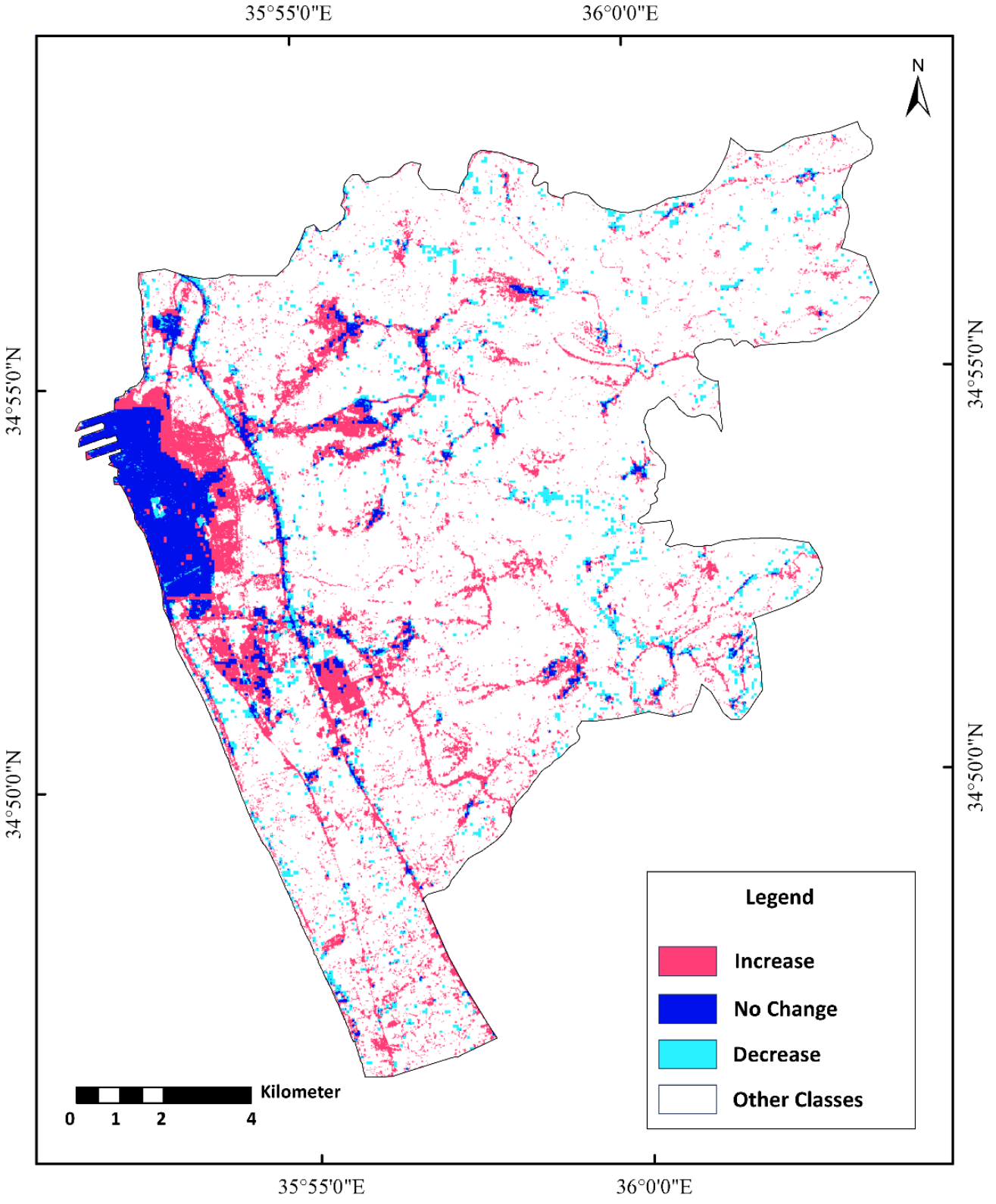

Figure 7. Built-up areas change from 1987 to 2019.

https://doi.org/10.48088/ejg.a.you.14.3.020.041

3.4. LULCC Environmental Impact

The environmental impact of LULCC was assessed using FCC (Figure 2). The results include five categories, namely (i) Positive Impact, (ii) Moderate Positive Impact, (iii) No Change, (iv) Moderate Negative Impact and (v) Negative Impact (Figure 3). The spatial distribution of these categories revealed significant observations. The study area mainly consisted of agricultural land, with most regions showing no change between 1987 and 2019. However, most spatial changes had negative environmental impacts, especially near built-up areas in the west, attributed to urban expansion. Meanwhile, the moderate negative impacts of spatial changes were concentrated in the hilly northeastern region. Nevertheless, a few areas had positive and moderate positive impacts, especially in the northeast.

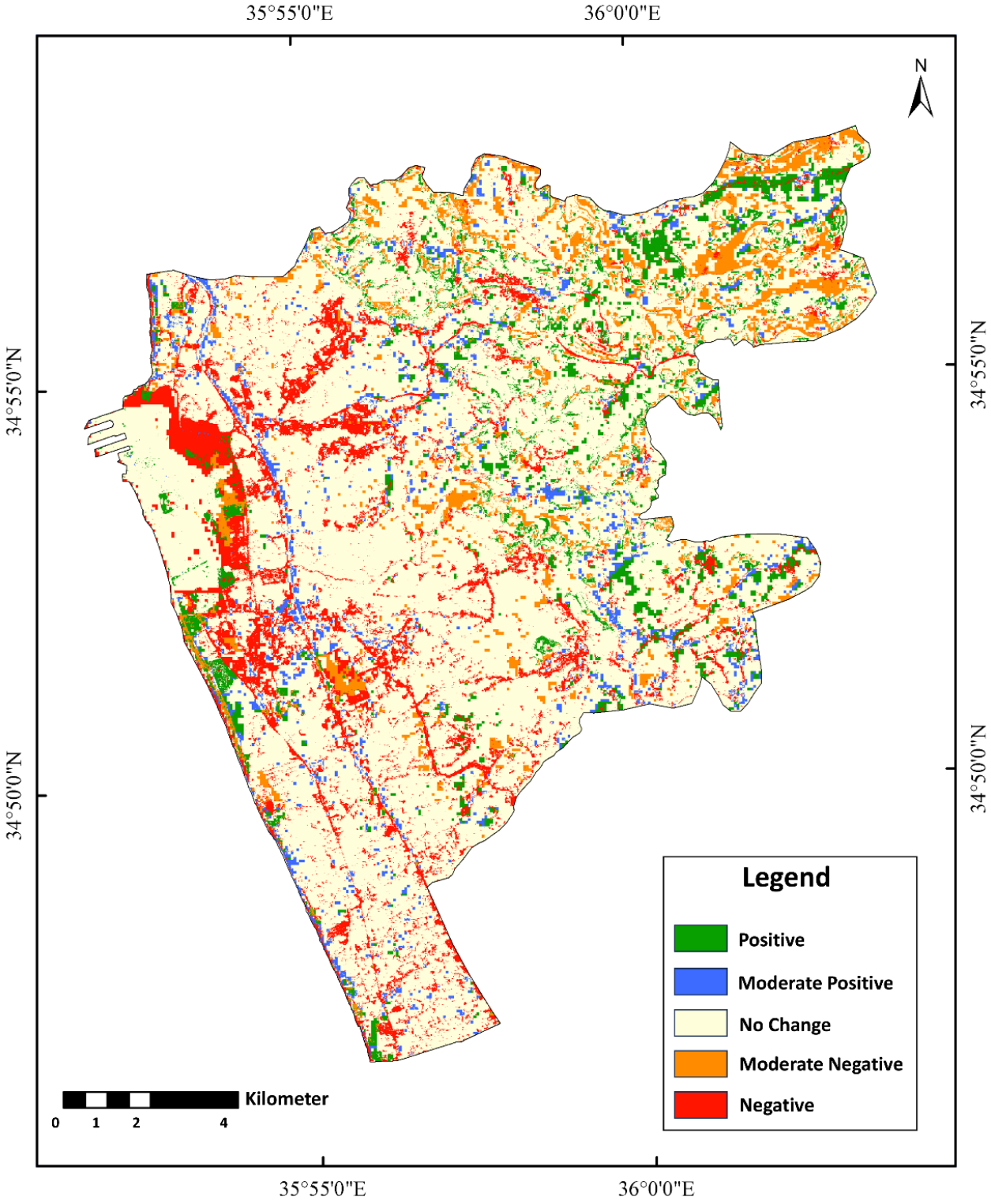

Figure 8. Environmental impact of LULCC from 1987 to 2019.

https://doi.org/10.48088/ejg.a.you.14.3.020.041

3.5. Spatio-temporal Extent of Built-up Areas

By applying the Equal To tool in the ArcMap GIS environment (Figure 2), the spatio-temporal extent of built-up areas was tracked between 1987 and 2019 (Figure 9). The analysis revealed notable spatial characteristics, with most of the expansion concentrated in the western region of the study area, indicating the rapid growth of Tartous City. In addition, the surrounding towns and villages have grown, transforming into larger peri-urban aggregates.

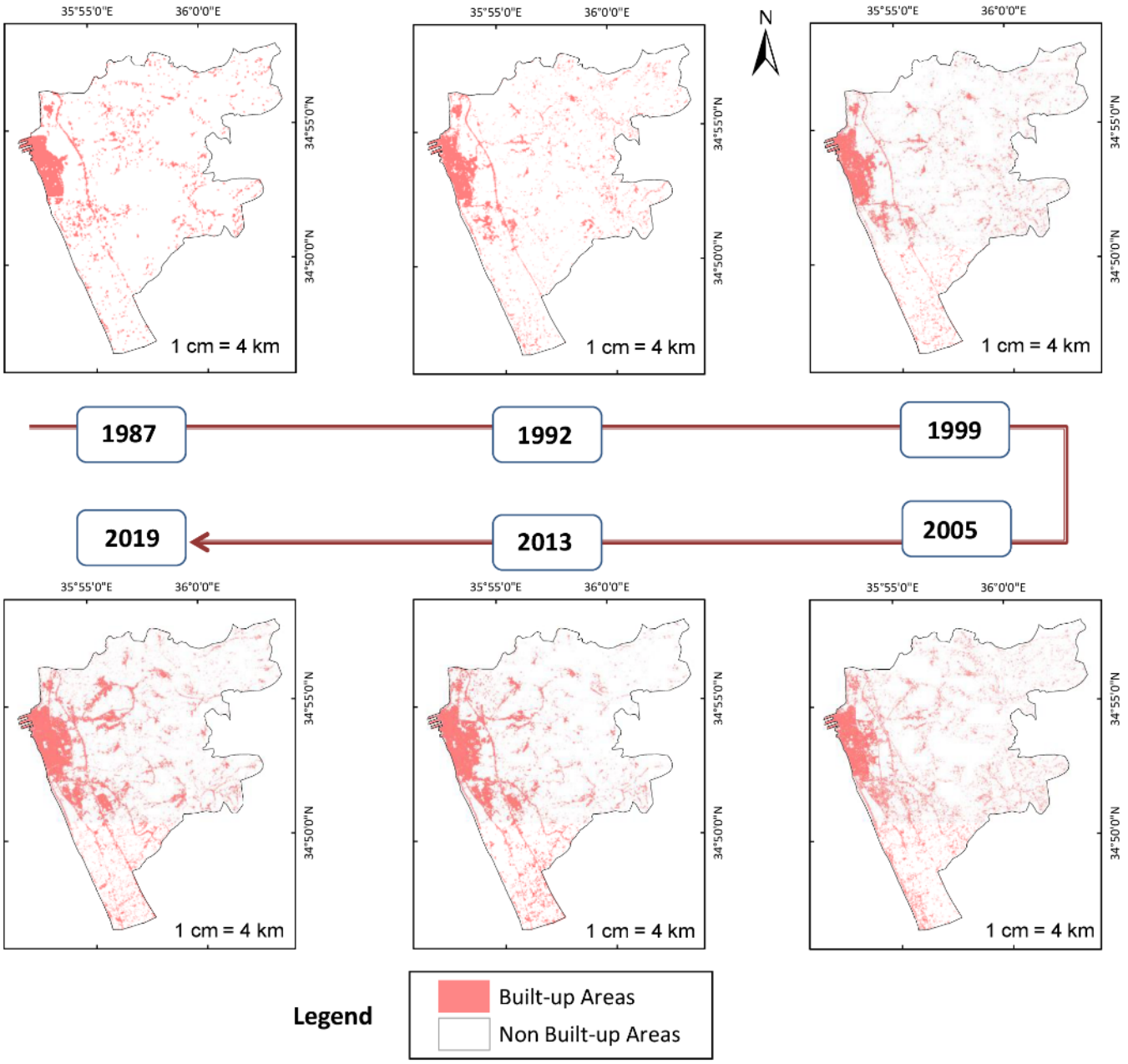

Figure 9. The spatio-temporal extent of built-up areas from 1987 to 2019.

4. Discussion

The results of LULC classification and PCC change detection indicate that Tartous has experienced significant LULC changes between 1987 and 2019. These results shed light on LULCC dynamics in Tartous and are consistent with previous research on Syria in general and Tartous in particular.

Agricultural land was identified as the predominant land use in this study, which is consistent with the fact that agriculture is the main economic activity in the region (Mohamed, 2021a; Rahmoun et al., 2018), with crops such as olives and citrus trees, wheat, vegetables (Faour & Fayad, 2014). Over the 32 years, agricultural land remained relatively stable, with some fluctuations observed in both periods. In particular, a decreasing trend was observed before the crisis, followed by an increasing trend during the crisis. This observation is consistent with the findings

of Abdo (2018), Rahmoun et al. (2018) and Mohamed (2021a), who also reported that agricultural land increased during the Syrian crisis in Tartous governorate. Abdo (2018) noted that this expansion was a response to the growing population and increasing livelihood demands of IDPs. Furthermore, the conversion of 84% of fallow land to agricultural land between 1987 and 2019 confirms this observation (Table 5). The PCC analysis revealed that the expansion of agricultural land was mainly at the expense of natural vegetation (Figure 10), especially in the northeast of the study area (Figure 4). The decline in agricultural land, on the other hand, occurred mainly near the built-up areas, especially near Tartous City (Figure 5 and Figure 10).

Natural vegetation, on the other hand, recorded a decrease of 4.7% during the crisis and 31.5% before. Several studies reported similar deterioration due to complex, interrelated factors, most notably the uncontrolled exploitation of land resources (Cazabat, 2018). For example, the cutting of firewood by local people to support their livelihoods is a common practise, especially in winter when fuel prices are high and the weather is cold (Abdo, 2018; Rahmoun et al., 2018), particularly during the Syrian crisis due to poor economic conditions (Mohamed, 2021a). The lack of forest guards (Abdo, 2018), the inefficiency of forest conservation management (Hammad et al., 2018), and frequent forest fires (Faour & Fayad, 2014; Mohamed et al., 2020) also contributed to the deterioration of natural vegetation. The PCC analysis showed that 60.4% of natural vegetation was lost to agricultural land, and 4.3% was converted to built-up areas (Table 5 and Figure 4). The results are consistent with other studies that have found a similar trend in Syria and Tartous. In particular, the growing population and influx of IDPs have likely led to the widespread conversion of natural vegetation into agricultural land for crop cultivation to intensify agricultural production and meet increasing demand (Abdo, 2018; Rahmoun et al., 2018). This practise was mainly observed in the hilly regions (Mohamed, 2021a) northeast of the study area (Figure 6 and Figure 10).

There was also a decline in water bodies despite their small extent. This change can be attributed to climate change and global warming, which have led to decreasing rainfall and increasing drought in Syria since the early 1980s (Zakhem & Hafez, 2010). Anthropogenic pressure on water resources also contributed to this decline (Al-Husban & Ayen, 2020; Cazabat, 2018; Müller et al., 2016). Water bodies experienced a greater de-crease of 60% during the crisis than before (Table 3). This observation is consistent with previous studies that identified the growing population and IDPs, increasing demand for water for domestic use or irrigation, water pollution and mismanagement as the leading causes of this decrease (Al-Husban & Ayen, 2020; Faour & Fayad, 2014; Müller et al., 2016).

No study explicitly and thoroughly mapped barren land and fallow land in the study area, likely due to the difficulties in modelling and classifying these two classes (Nguyen et al., 2021; Wallace et al., 2017). Fallow land is arable land that is left uncultivated for at least one season, sometimes up to 10 years, to allow soil fertility to regenerate (Nielsen & Calderón, 2011; Zambon et al., 2018). In this study, fallow land refers to cropland left unseeded for more than one year and transitional areas between natural vegetation and agricultural land (Table 2). These lands fluctuated and are mainly observed amidst agricultural areas, especially near natural vegetation. Their decrease (-80%) during the crisis compared to the increase (+16%) before the crisis refers to the significant conversion of former fallow land into expanded agricultural land during the crisis, especially in the northeastern region (Figure 4 and Figure 10). Barren land, on the other hand, refers to exposed uncultivable land and transitional areas from agricultural land to built-up areas. They are dynamic and characterised by continuous changes, with the area decreasing throughout the study period. However, during the crisis, their area decreased faster (-71.5%) than before, probably due to the rapid increase of built-up areas during the crisis (Abdo, 2018; CBS, 2023; Mohamed, 2021a; Rahmoun et al., 2018). The PCC analysis showed that 43% of barren land was converted to built-up areas (Table 5 and Figure 4), indicating a significant expansion of built-up areas, with a spatial concentration around Tar-tous City and nearby towns in the western part of the study area (Figure 7 and Figure 10).

According to Table 3, the growth of built-up areas almost doubled between 1987 and 2019 due to rapid population growth, rural depopulation and the influx of IDPs (Mohamed, 2021a). This necessitated the acquisition of more land for horizontal expansion to meet the demands of urban development (Abdo, 2018). It was reported that the population density in the narrow coastal strip is almost 20 times higher than the national average and six times higher than the average population density in other interior parts of the coastal region (CBS, 2023; Mohamed, 2021a). The PCC analysis and spatio-temporal modelling revealed that the growth of built-up areas could be divided into two spatial patterns: (i) the expansion of Tartous City in the western part of the study area and (ii) the growth of towns and villages scattered across the study area (Figure 7 and Figure 9).

Tartous City is the largest urban pole in the study area (Figure 10), having grown steadily from 1987 to 2019 (Figure 9). In 1987, built-up areas were limited to Tartous City and a few scattered villages to the east. During this period, built-up areas expanded; Tartous city became larger, villages became towns, and new aggregates emerged. It has been suggested that Tartous City expanded mainly towards the east and south while surrounding villages and towns grew along road networks connecting Tartous to other urban centres within and outside the governorate. Overall, the results indicate significant growth in Tartous City and other urban aggregates in the study area, with this growth having a spatial direction and being related to several variables, such as the road network and geographical constraints. Although no study has thoroughly investigated the spatio-temporal extent of built-up areas in the Tartous, available studies confirm urban expansion in the area (Abdo, 2018; Mohamed, 2021b, 2021a; Mohamed et al., 2020; Rahmoun et al., 2018).

Monitoring LULCC dynamics in Tartous provides important insights into potential drivers. While natural factors, particularly climate change and global warming, cannot be ignored, anthropogenic pressure has been identified as the most important force. The results suggest that anthropo-genic pressures can manifest in proximate and underlying forms. Before the crisis, LULCC was primarily driven by underlying anthropogenic pres-sure caused by national socio-economic development and various cultural and biophysical factors. In contrast, anthropogenic pressures became more proximate during the crisis and directly affected LULCC at the local level. This was due to a combination of slow and rapid forces, including the growing local population, the influx of IDPs, the war and the accompanying economic shock. These findings are consistent with previous research identifying similar forces as key drivers of LULCC in Syria during the crisis and before (Abdo, 2018; Abeed et al., 2021; Al-Husban & Ayen, 2020; Cazabat, 2018; Hammad et al., 2018; Heidarlou et al., 2020; Jaafar et al., 2015; Landholm et al., 2019; Mohamed et al., 2020; Mohamed, 2021b, 2021a; Müller et al., 2016; Rahmoun et al., 2018).

Although few studies investigated the environmental impacts of LULCC in the study area, studies conducted in other parts of Syria and other countries support our findings. Most LULCC had negative environmental impacts, with a spatial concentration near built-up areas, especially around Tartous City in the western part of the study area (Figure 8). The expansion of built-up areas at the expense of surrounding agricultural land, natural vegetation, and water bodies leads to environmental degradation and deprives these LULCs of their environmental quality and ecosystem services (Fang et al., 2022; Pauleit et al., 2005; Sharma et al., 2023). Such unplanned urbanisation could alter land-atmosphere energy exchange (Parveen et al., 2018) and affect microclimate and local land surface temperature (Krishnan & Firoz, 2021; Rahaman et al., 2020). This can lead to more greenhouse gases and increased pollution (Santos et al., 2021). The moderate negative impacts were mainly observed in the hilly

region in the northeast (Figure 8), where ecosystems are considered sensitive to human activities and global change (Li & Deng, 2017). The main cause of these impacts is deforestation, which is a concern given the high environmental quality of natural vegetation and forest areas (Chazdon et al., 2020; Pauleit et al., 2005). Several studies reported likely consequences of this degradation, such as soil erosion (Abdo, 2018; Alsafadi et al., 2022; Mohammed et al., 2020), loss of soil organic carbon (SOC) (Chazdon et al., 2020; Fang et al., 2022; Winowiecki et al., 2015), increased carbon dioxide (CO2) (Santos et al., 2021), reduced water conservation (Li & Deng, 2017), increased vulnerability to flooding and other hazards (Abdo, 2020; Li & Deng, 2017), loss of natural habitats and biodiversity (Butt et al., 2015; Mohamed et al., 2020). However, positive im-pacts have been observed in a few areas in the northeast, likely indicating minor restoration of natural vegetation on previously agricultural land. Restoration of natural vegetation contributes to the conservation of biodiversity and the provision of various ecosystem services. To some extent, it can alleviate local environmental degradation, as evidenced by several studies (Chazdon et al., 2020; Fang et al., 2022; Hao & Ren, 2009; Mohamed, 2021a; Winowiecki et al., 2015).

Figure 10. Field photos (taken by colleagues of the first author between 9 and 10 August 2020). (a) Agricultural land: olive tree plantation on account of natural vegetation, (b) Fallow land: transitional land; natural vegetation to agricultural land, (c) Natural vegetation, (d) Built-up areas: urban expansion on account of agricultural land, (e) Barren land: transitional land; agricultural land to built-up areas, (f) Built-up areas: Tartous City.

5. Conclusions

Tartous, a relatively small governorate in the coastal region of Syria, experienced a significant influx of IDPs, resulting in the highest displacement burden in the country. The LULCC in Tartous underwent significant changes from 1987 to 2019, with the driving forces of the LULCC during the crisis differing from those before. It is suggested that the growing population, economic recession and war played an important role in this change, leading to increasing controversy between people and land.

Recent demands to improve livelihoods and promote socio-economic levels in Syria, especially in Tartous, led to a depletion of land resources. Natural vegetation, particularly in the northeastern hills, experienced significant degradation, declining by 40% between 1987 and 2019,

with 60% of this decline due to agricultural expansion. Built-up Areas in the west has doubled over the study period from 18 km2 in 1987 to 34 km2 in 2019, with negative environmental impacts. Despite the decline in agricultural land due to urbanisation, the conversion of fallow land and natural vegetation resulted in a net increase in agricultural use, especially during the crisis. Thus, agricultural land remains the predominant land use in the study area, accounting for about 74% to 75% of the study area and representing the main economic activity of the local population. Such LULCC, characterised by deforestation, agricultural expansion and urban sprawl, has negative impacts on the environment, such as weakening soil and water conservation capacity, reducing vegetation productivity and increasing the risk of geohazards occurrence, putting high pressure on livelihood improvement. Therefore, there is an urgent need to pay special attention to war-affected regions. Multi-level regional plans are now essential to regulate the overexploitation of land resources and to contribute effectively to environmental conservation and sustainable land management practises. At the same time, however, it is crucial that these plans also prioritise local needs for prosperous livelihoods in such contexts.

Funding: This research received no external funding.

Data Availability Statement: Data might be available upon a reasonable request.

Acknowledgements: The first author would like to thank the Indian Council for Cultural Relations (ICCR) in India, University of Tartous and Ministry of Higher Education and Scientific Research in Syria for their moral and academic support.

Conflicts of Interest: The authors declare no conflict of interest.

References

Abburu, S., & Babu Golla, S. (2015). Satellite Image Classification Methods and Techniques: A Review. *International Journal of Computer Applications,* 119(8), 20–25. https://doi.org/10.5120/21088-3779

Abdo, H. G. (2018). Impacts of war in Syria on vegetation dynamics and erosion risks in Safita area, Tartous, Syria. *Regional Environmental Change*, 18(6), 1707–1719. https://doi.org/10.1007/s10113-018-1280-3

Abdo, H. G. (2020). Evolving a total-evaluation map of flash flood hazard for hydro-prioritization based on geohydromorphometric parameters and GIS–RS manner in Al-Hussain river basin, Tartous, Syria. *Natural Hazards*, 104(1), 681–703. https://doi.org/10.1007/s11069-020-04186-3

Abeed, R., Clerbaux, C., Clarisse, L., Damme, M. van, Coheur, P. F., & Safieddine, S. (2021). A space view of agricultural and industrial changes during the Syrian civil war. *Elementa: Science of the Anthropocene*, 9(1), 1–13. https://doi.org/10.1525/elementa.2021.000041

Aide, T. M., & Grau, H. R. (2004). Globalization, migration, and latin american ecosystems. *Science,* 305(5692), 1915–1916. https://doi.org/10.1126/science.1103179

Al-Fares, W. (2013). Historical Land Use/Land Cover Classification using Remote Sensing—A Case Study of the Euphrates River Basin in Syria (1st ed.). Springer Cham. https://doi.org/10.1007/978-3-319-00624-6

Al-Husban, Y., & Ayen, A. (2020). The impact of the syrian civil war on land use / land cover in al-yarmouk basin during 2010–2018. Geography, Environment, *Sustainability*, 13(2), 147–153. https://doi.org/10.24057/2071-9388-2018-73

Alsafadi, K., Bi, S., Abdo, H. G., Al Sayah, M. J., Ratonyi, T., Harsanyi, E., & Mohammed, S. (2022). Spatial–temporal dynamic impact of changes in rainfall erosivity and vegetation coverage on soil erosion in the Eastern Mediterranean. *Environmental Science and Pollution Research*. https://doi.org/10.1007/s11356-022-24012-6

Anand, A. (2012). Accuracy Assessment. In Remote Sensing and Image Interpretation (pp. 59–77). Indira Gandhi National Open University (IGNOU). https://www.researchgate.net/publication/324943246_UNIT_14_ACCURACY_ASSESSMENT

Attri, P., Chaudhry, S., & Sharma, S. (2015). Remote Sensing & GIS based Approaches for LULC Change Detection-A Review. *International Journal of Current Engineering and Technology*, 5(5), 3126–3137. https://www.researchgate.net/publication/325145097_Remote_Sensing_GIS_based_Approaches_for_LULC_Change_Detection_-_A_Review

Butt, A., Shabbir, R., Ahmad, S. S., & Aziz, N. (2015). Land use change mapping and analysis using Remote Sensing and GIS: A case study of Simly watershed, Islamabad, Pakistan. *Egyptian Journal of Remote Sensing and Space Science*, 18, 251–259. https://doi.org/10.1016/j.ejrs.2015.07.003

Cazabat, C. (2018). The Ripple Effect: Multidimensional Impacts of Internal Displacement (J. Lennard (ed.); Issue October). https://www.internal-displacement.org/publications/the-ripple-effect-economic-impacts-of-internal-displacement

CBS. (2023). Statistical Abstract for Years: 2010, 2017, 2018, and 2019. Statistical Abstract. http://cbssyr.sy/yearbook-EN.htm

Chaikaew, P. (2019). Land Use Change Monitoring and Modelling using GIS and Remote Sensing Data for Watershed Scale in Thailand. In L. C. Loures (Ed.), Land Use - Assessing the Past, Envisioning the Future (pp. 165–181). IntechOpen. https://doi.org/10.5772/intechopen.79167

Chakraborty, A., Sachdeva, K., & Joshi, P. K. (2017). A Reflection on Image Classifications for Forest Ecology Management: Towards Landscape Mapping and Monitoring. In Handbook of Neural Computation (First, pp. 67–85). Academic Press. https://doi.org/10.1016/B978-0-12-811318-9.00004-1

Chazdon, R. L., Lindenmayer, D., Guariguata, M. R., Crouzeilles, R., Rey Benayas, J. M., & Lazos Chavero, E. (2020). Fostering natural forest regeneration on former agricultural land through economic and policy interventions. *Environmental Research Letters*, 15(043002). https://doi.org/10.1088/1748-9326/ab79e6

Chen, D. M., & Stow, D. (2002). The effect of training strategies on supervised classification at different spatial resolutions. *Photogrammetric Engineering and Remote Sensing,* 68(11), 1155–1161. https://www.researchgate.net/publication/265659743_The_Effect_of_Training_Strategies_on_Supervised_Classification_at_Different_Spatial_Resolutions

Congalton, R. G., & Green, K. (2019). Assessing the Accuracy of Remotely Sensed Data: Principles and Practices (3rd ed.). CRC Press. https://doi.org/https://doi.org/10.1201/9780429052729

De Pauw, E., Oberle, A., & Zöbisch, M. (2004). Overview of land cover and land use in Syria: base year 1989/1990 (Issue 47). https://agris.fao.org/agris-search/search.do?recordID=QV2005000042

Doocy, S., Lyles, E., Delbiso, T. D., Robinson, C. W., & The IOCC/GOPA Study Team. (2015). Internal displacement and the Syrian crisis: An analysis of trends from 2011-2014. *Conflict and Health*, 9(33), 1–11. https://doi.org/10.1186/s13031-015-0060-7

Dudley, J. P., Ginsberg, J. R., Plumptre, A. J., Hart, J. A., & Campos, L. C. (2002). Effects of war and civil strife on wildlife and wildlife habitats. *Conservation Biology*, 16(2), 319–329. https://doi.org/10.1046/j.1523-1739.2002.00306.x

Eklund, L., Degerald, M., Brandt, M., Prishchepov, A. V., & Pilesjö, P. (2017). How conflict affects land use: Agricultural activity in areas seized by the Islamic State. *Environmental Research Letters*, 12(054004). https://doi.org/10.1088/1748-9326/aa673a

El-Hattab, M. M. (2016). Applying post classification change detection technique to monitor an Egyptian coastal zone (Abu Qir Bay). Egyptian *Journal of Remote Sensing and Space Science*, 19(1), 23–36. https://doi.org/10.1016/j.ejrs.2016.02.002

Enderle, D. I. ., & Weih Jr., R. C. (2005). Integrating Supervised and Unsupervised Classification Methods to Develop a More Accurate Land Cover Classification. *Journal of the Arkansas Academy of Science*, 59. https://scholarworks.uark.edu/jaas/vol59/iss1/10/

EOS. (2023). NASA's Earth Observing System. https://eos.com/make-an-analysis/color-infrared/

ESA. (2023). The European Space Agency ESA - SENTINEL-2 MISSION GUIDE. https://sentinel.esa.int/web/sentinel/missions/sentinel-2

ESRI. (2023a). Accuracy Assessment for Image Classification. Environmental Systems Research Institute. https://desktop.arcgis.com/en/arcmap/latest/manage-data/raster-and-images/accuracy-assessment-for-image-classification.htm

ESRI. (2023b). Equal To (Spatial Analyst). Environmental Systems Research Institute. https://pro.arcgis.com/en/pro-app/latest/tool-reference/spatial-analyst/equal-to.htm

ESRI. (2023c). How the relational math tools work. Environmental Systems Research Institute. https://pro.arcgis.com/en/pro-app/latest/tool-reference/spatial-analyst/h-how-the-relational-math-tools-work.htm

Fang, Z., Ding, T., Chen, J., Xue, S., Zhou, Q., Wang, Y., Wang, Y., Huang, Z., & Yang, S. (2022). Impacts of land use/land cover changes on ecosystem services in ecologically fragile regions. *Science of The Total Environment*, 831(154967). https://doi.org/10.1016/j.scitotenv.2022.154967

Faour, G., & Fayad, A. (2014). Water Environment in the Coastal Basins of Syria - Assessing the Impacts of the War. Environmental Processes, 1, 533–552. https://doi.org/10.1007/s40710-014-0043-5

Ferraris, V., Dobigeon, N., Wei, Q., & Chabert, M. (2017). Robust Fusion of Multiband Images With Different Spatial and Spectral Resolutions for Change Detection. *IEEE Transactions on Computational Imaging*, 3(2), 175–186. https://doi.org/10.1109/tci.2017.2692645

Finegold, Y., & Ortmann, A. (2016). Map accuracy assessment and area estimation : a practical guide. In National forest monitoring assessment working paper (46/E). Food and Agriculture Organization of the United Nations (FAO). https://www.fao.org/documents/card/en?details=e5ea45b8-3fd7-%2F

Foody, G. M., & Mathur, A. (2004). Toward intelligent training of supervised image classifications: Directing training data acquisition for SVM classification. *Remote Sensing of Environment*, 93(1–2), 107–117. https://doi.org/10.1016/j.rse.2004.06.017

Geist, H. J., & Lambin, E. F. (2002). Proximate causes and underlying driving forces of tropical deforestation. *BioScience,* 52(2), 143–150. https://doi.org/10.1641/0006-3568(2002)052[0143:PCAUDF]2.0.CO;2

Halder, J. C. (2018). Population change and land use dynamics: A case study of Paschim Medinipur District, West Bengal, India. *European Journal of Geography,* 9(3), 23–44. https://www.eurogeojournal.eu/index.php/egj/article/view/45

Hammad, M., Mucsi, L., & van Leeuwen, B. (2018). Land Cover Change Investigation in the Southern Syrian Coastal Basins During the Past 30-Years Using Landsat Remote Sensing Data. *Journal of Environmental Geography*, 11(1–2), 45–51. https://doi.org/10.2478/jengeo-2018-0006

Hao, H. mei, & Ren, Z. yuan. (2009). Land Use/Land Cover Change (LUCC) and Eco-Environment Response to LUCC in Farming-Pastoral Zone, China. *Agricultural Sciences in China*, 8(1), 91–97. https://doi.org/10.1016/S1671-2927(09)60013-4

Hassan, Z., Shabbir, R., Ahmad, S. S., Malik, A. H., Aziz, N., Butt, A., & Erum, S. (2016). Dynamics of land use and land cover change (LULCC) using geospatial techniques: a case study of Islamabad Pakistan. SpringerPlus, 5(812). https://doi.org/10.1186/s40064-016-2414-z

Heidarlou, H. B., Shafiei, A. B., Erfanian, M., Tayyebi, A., & Alijanpour, A. (2020). Armed conflict and land-use changes: Insights from Iraq-Iran war in Zagros forests. *Forest Policy and Economics*, 118(102246). https://doi.org/10.1016/j.forpol.2020.102246

Hu, C., Song, M., & Zhang, A. (2023). Dynamics of the eco-environmental quality in response to land use changes in rapidly urbanizing areas: A case study of Wuhan, China from 2000 to 2018. *Journal of Geographical Sciences*, 33, 245–265. https://doi.org/10.1007/s11442-023-2081-2

Ibrahim, W. Y., Batzli, S., & Menzel, W. P. (2014). Agricultural policy effects on land cover and land use over 30 years in Tartous, Syria, as seen in Landsat imagery. *Journal of Applied Remote Sensing*, 8(083506). https://doi.org/10.1117/1.jrs.8.083506

IPCC. (2019). Climate Change and Land: An IPCC Special Report on climate change, desertification, land degradation, sustainable land management, food security, and greenhouse gas fluxes in terrestrial ecosystems. https://www.ipcc.ch/srccl/

Jaafar, H. H., Zurayk, R., King, C., Ahmad, F., & Al-Outa, R. (2015). Impact of the Syrian conflict on irrigated agriculture in the Orontes Basin. *International Journal of Water Resources Development,* 31(3), 436–449. https://doi.org/10.1080/07900627.2015.1023892

Jain, S. ., & Singh, V. . (2003). Reservoir sedimentation. In Developments in Water Science (Vol. 51, Issue C, pp. 681–741). Elsevier. https://doi.org/10.1016/S0167-5648(03)80066-7

Kafy, A. Al, Rahman, M. S., Faisal, A. Al, Hasan, M. M., & Islam, M. (2020). Modelling future land use land cover changes and their impacts on land surface temperatures in Rajshahi, Bangladesh. *Remote Sensing Applications: Society and Environment*, 18(100314). https://doi.org/10.1016/j.rsase.2020.100314

Khandve, P. V, & Mokadam, A. M. (2011). Application of GIS in Environmental Engineering. National Conference on Environment Pollution and Management, 244–250. https://www.researchgate.net/publication/292695439_Application_of_GIS_in_Environmental_Engineering

Kraemer, H. C. (2015). Kappa Coefficient. Wiley StatsRef: Statistics Reference Online, 1–4. https://doi.org/10.1002/9781118445112.stat00365.pub2

Krishnan, S., & Firoz, M. (2021). Impact of land use and land cover change on the environmental quality of a region: A case of Ernakulam district in Kerala, India. *Regional Statistics*, 11(2), 102–135. https://doi.org/10.15196/RS110205

Kulo, N. (2018). Benefits of the Remote Sensing Data Integration. 1st Western Balkan Conference on GIS, Mine Surveying, Geodesy and Geomatic, 0–14. https://www.researchgate.net/publication/329443299_Benefits_of_the_Remote_Sensing_Data_Integration

Lam, N. S. N. (2008). Methodologies for mapping land cover/land use and its change. *Advances in Land Remote Sensing: System, Modeling, Inversion and Application*, 341–367. https://doi.org/10.1007/978-1-4020-6450-0_13

Lambin, E. F., & Meyfroidt, P. (2011). Global land use change, economic globalization, and the looming land scarcity. Proceedings of the National Academy of Sciences of the United States of America (PNAS), 108(9), 3465–3472. https://doi.org/10.1073/pnas.1100480108

Lambin, E. F., Turner, B. L., Geist, H. J., Agbola, S. B., Angelsen, A., Bruce, J. W., Coomes, O. T., Dirzo, R., Fischer, G., Folke, C., George, P. S., Homewood, K., Imbernon, J., Leemans, R., Li, X., Moran, E. F., Mortimore, M., Ramakrishnan, P. S., Richards, J. F., … Xu, J. (2001). The causes

of land-use and land-cover change: Moving beyond the myths. *Global Environmental Change*, 11(4), 261–269. https://doi.org/10.1016/S0959-3780(01)00007-3

Landholm, D. M., Pradhan, P., & Kropp, J. P. (2019). Diverging forest land use dynamics induced by armed conflict across the tropics. *Global Environmental Change*, 56, 86–94. https://doi.org/10.1016/j.gloenvcha.2019.03.006

Li, A., & Deng, W. (2017). Land use/cover change and its eco-environmental responses in Nepal: An overview. In W. Zhao, A. Li, & W. Deng (Eds.), Land use/cover change and its eco-environmental responses in Nepal (pp. 1–13). *Springer Geography*. https://doi.org/10.1007/978-981-10-2890-8_1

Lu, D., & Weng, Q. (2007). A survey of image classification methods and techniques for improving classification performance. *International Journal of Remote Sensing*, 28(5), 823–870. https://doi.org/10.1080/01431160600746456

Mallupattu, P. K., & Sreenivasula Reddy, J. R. (2013). Analysis of land use/land cover changes using remote sensing data and GIS at an Urban Area, Tirupati, India. *The Scientific World Journal*, 2013(268623), 1–7. https://doi.org/10.1155/2013/268623

McGlynn, B. L., & Seibert, J. (2003). Distributed assessment of contributing area and riparian buffering along stream networks. *Water Resources Research,* 39(4), 1–7. https://doi.org/10.1029/2002WR001521

McHugh, M. L. (2012). Lessons in biostatistics interrater reliability : the kappa statistic. *Biochemica Medica*, 22(3), 276–282. https://pubmed.ncbi.nlm.nih.gov/23092060/

Mohajane, M., Essahlaoui, A., Oudija, F., Hafyani, M. El, Hmaidi, A. El, Ouali, A. El, Randazzo, G., & Teodoro, A. C. (2018). Land use/land cover (LULC) using landsat data series (MSS, TM, ETM+ and OLI) in azrou forest, in the central middle atlas of Morocco. *Environments,* 5(12), 1–16. https://doi.org/10.3390/environments5120131

Mohamed, M. A. (2021a). An assessment of forest cover change and its driving forces in the syrian coastal region during a period of conflict, 2010 to 2020. *Land,* 10(2), 1–25. https://doi.org/10.3390/land10020191

Mohamed, M. A. (2021b). Spatiotemporal impacts of urban land use/land cover changes on land surface temperature: A comparative study of damascus and aleppo (syria). *Atmosphere,* 12(8), 1–26. https://doi.org/10.3390/atmos12081037

Mohamed, M. A., Anders, J., & Schneider, C. (2020). Monitoring of Changes in Land Use/Land Cover in Syria from 2010 to 2018 Using Multitemporal Landsat Imagery and GIS. *Land,* 9(7). https://doi.org/10.3390/land9070226

Mohammed, S., Abdo, H. G., Szabo, S., Pham, Q. B., Holb, I. J., Linh, N. T. T., Anh, D. T., Alsafadi, K., Mokhtar, A., Kbibo, I., Ibrahim, J., & Rodrigo-Comino, J. (2020). Estimating human impacts on soil erosion considering different hillslope inclinations and land uses in the coastal region of syria. *Water,* 12(10). https://doi.org/10.3390/w12102786

Morgan, G. R., & Hodgson, M. E. (2021). A Post-Classification Change Detection Model with Confidences in High Resolution Multi-Date sUAS Imagery in Coastal South Carolina. *International Journal of Remote Sensing*, 42(11), 4309–4336. https://doi.org/10.1080/01431161.2021.1890266

Mosammam, H. M., Nia, J. T., Khani, H., Teymouri, A., & Kazemi, M. (2017). Monitoring land use change and measuring urban sprawl based on its spatial forms: The case of Qom city. *Egyptian Journal of Remote Sensing and Space Science*, 20(1), 103–116. https://doi.org/10.1016/j.ejrs.2016.08.002

Müller, M. F., Yoon, J., Gorelick, S. M., Avisse, N., & Tilmant, A. (2016). Impact of the Syrian refugee crisis on land use and transboundary freshwater resources. Proceedings of the National Academy of Sciences of the United States of America (PNAS), 113(52), 14932–14937. https://doi.org/10.1073/pnas.1614342113

Murillo-Sandoval, P. J., Gjerdseth, E., Correa-Ayram, C., Wrathall, D., Van Den Hoek, J., Dávalos, L. M., & Kennedy, R. (2021). No peace for the forest: Rapid, widespread land changes in the Andes-Amazon region following the Colombian civil war. *Global Environmental Change*, 69(102283). https://doi.org/10.1016/j.gloenvcha.2021.102283

NASA. (2023a). ASTER - Advanced Spaceborne Thermal Emission and Reflection Radiometer. TERRA. https://terra.nasa.gov/about/terra-instruments/aster

NASA. (2023b). How to Interpret Common False Color Images. Earth Observatory. https://earthobservatory.nasa.gov/features/FalseColor/page6.php

Nguyen, C. T., Chidthaisong, A., Diem, P. K., & Huo, L.-Z. (2021). A Modified Bare Soil Index to Identify Bare Land Features during Agricultural Fallow-Period in Southeast Asia Using Landsat 8. Land, 10(3). https://doi.org/10.3390/land10030231

Nielsen, D. C., & Calderón, F. J. (2011). Fallow Effects on Soil. In J. L. Hatfield & T. J. Sauer (Eds.), Soil Management: Building a Stable Base for Agriculture (pp. 287–300). American Society of Agronomy, Soil Science Society of America. https://doi.org/10.2136/2011.soilmanagement.c19

OCHA. (2014). Syrian Arab Republic: Governate Profiles. In United Nations Office for the Coordination of Humanitarian Affairs. https://www.unocha.org/

Omusotsi, O. G. (2019). Role of GIS as a Tool for Environmental Planning and Management. *International Journal of Research in Environmental Science (IJRES),* 5(1). https://doi.org/10.20431/2454-9444.0501002

Pandian, M., Rajagopal, N., Sakthivel, G., & Amrutha, D. . (2014). Land Use and Land Cover Change Detection Using Remote Sensing and GIS in Parts of Coimbatore and Tiruppur Districts, Tamil Nadu, India. *International Journal of Remote Sensing & Geoscience (IJRSG),* 3(1). https://www.researchgate.net/publication/266210112_LAND_USE_AND_LAND_COVER_CHANGE_DETECTION_USING_REMOTE_SENSING_AND_GIS_IN_PARTS_OF_COIMBATORE_AND_TIRUPPUR_DISTRICTS_TAMIL_NADU_INDIA

Park, N., Kim, Y., & Kwak, G.-H. (2019). An Overview of Theoretical and Practical Issues in Spatial Downscaling of Coarse Resolution Satellite-derived Products. *Korean Journal of Remote Sensing*, 35(4), 589–607. https://doi.org/10.7780/kjrs.2019.35.4.8

Parveen, S., Basheer, J., & Praveen, B. (2018). a Literature Review on Land Use Land Cover Changes. *International Journal of Advanced Research*, 6(7), 1–6. https://doi.org/10.21474/ijar01/7327

Pauleit, S., Ennos, R., & Golding, Y. (2005). Modeling the environmental impacts of urban land use and land cover change—a study in Merseyside, UK. *Landscape and Urban Planning*, 71(2–4), 295–310. https://doi.org/10.1016/j.landurbplan.2004.03.009

Pickering, J., Tyukavina, A., Khan, A., Potapov, P., Adusei, B., Hansen, M. C., & Lima, A. (2021). Using multi-resolution satellite data to quantify land dynamics: Applications of planetscope imagery for cropland and tree-cover loss area estimation. *Remote Sensing,* 13(11). https://doi.org/10.3390/rs13112191

Porwal, S., & Katiyar, S. K. (2014). Performance evaluation of various resampling techniques on IRS imagery. 7th International Conference on Contemporary Computing, (IC3), 489–494. https://doi.org/10.1109/IC3.2014.6897222

Rahaman, S., Kumar, P., Chen, R., Meadows, M. E., & Singh, R. B. (2020). Remote Sensing Assessment of the Impact of Land Use and Land Cover Change on the Environment of Barddhaman District, West Bengal, India. *Frontiers in Environmental Science*, 8. https://doi.org/10.3389/fenvs.2020.00127

Rahmoun, T., Zhao, W., Hammad, M., & Hassan, M. (2018). Ruralization vs. Urbanization Sprawl as Guiding Regional Planning: Development Scenario for Rivers Watershed in the Southern Syrian Coastal Region. *IOP Conference Series: Earth and Environmental Science*, 151(012033). https://doi.org/10.1088/1755-1315/151/1/012033

Rudel, T. K., Coomes, O. T., Moran, E., Achard, F., Angelsen, A., Xu, J., & Lambin, E. (2005). Forest transitions: Towards a global understanding of land use change. *Global Environmental Change*, 15(1), 23–31. https://doi.org/10.1016/j.gloenvcha.2004.11.001

Rwanga, S. S., & Ndambuki, J. M. (2017). Accuracy Assessment of Land Use/Land Cover Classification Using Remote Sensing and GIS. *International Journal of Geosciences*, 8(4). https://doi.org/10.4236/ijg.2017.84033

Santos, M. J., Smith, A. B., Dekker, S. C., Eppinga, M. B., Leitão, P. J., Moreno-Mateos, D., Morueta-Holme, N., & Ruggeri, M. (2021). The role of land use and land cover change in climate change vulnerability assessments of biodiversity: a systematic review. *Landscape Ecology,* 36, 3367–3382. https://doi.org/10.1007/s10980-021-01276-w

Schowengerdt, R. A. (2007). Thematic Classification. In Remote Sensing - Models and Methods for Image Processing (Third, pp. 387–456, XXVII–XXXIII). Academic Press. https://doi.org/10.1016/b978-012369407-2/50012-7

Seto, K. C., Güneralp, B., & Hutyra, L. R. (2012). Global forecasts of urban expansion to 2030 and direct impacts on biodiversity and carbon pools. Proceedings of the National Academy of Sciences of the United States of America (PNAS), 109(40), 16083–16088. https://doi.org/10.1073/pnas.1211658109

Sharma, S., Hussain, S., & Singh, A. N. (2023). Impact of land use and land cover on urban ecosystem service value in Chandigarh, India: a GIS-based analysis. *Journal of Urban Ecology,* 9(1), 1–12. https://doi.org/10.1093/jue/juac030

Sisodia, P. S., Tiwari, V., & Kumar, A. (2014). Analysis of Supervised Maximum Likelihood Classification for remote sensing image. International Conference on Recent Advances and Innovations in Engineering, ICRAIE 2014, 1–4. https://doi.org/10.1109/ICRAIE.2014.6909319

Talukdar, S., Singha, P., Mahato, S., Shahfahad, Pal, S., Liou, Y.-A., & Rahman, A. (2020). Land-Use Land-Cover Classification by Machine Learning Classifiers for Satellite Observations — A Review. *Remote Sensing,* 12(7). https://doi.org/10.3390/rs12071135

Tucker, C. J., Grant, D. M., & Dykstra, J. D. (2004). NASA's global orthorectified landsat data set. *Photogrammetric Engineering and Remote Sensing,* 70(3), 313–322. https://doi.org/10.14358/PERS.70.3.313

Twisa, S., & Buchroithner, M. F. (2019). Land-use and land-cover (LULC) change detection in Wami river basin, Tanzania. *Land,* 8(9). https://doi.org/10.3390/land8090136

United Nations. (2019). World Urbanization Prospects: The 2018 Revision (ST/ESA/SER.A/420). In Department of Economic and Social Affairs, Population Division (2019). https://population.un.org/wup/Publications/

USGS. (2023a). Common Landsat Band Combinations. United States Geological Survey. https://www.usgs.gov/media/images/common-landsat-band-combinations

USGS. (2023b). USGS EROS Archive - Digital Elevation - Shuttle Radar Topography Mission (SRTM) 1 Arc-Second Global. United States Geological Survey. https://www.usgs.gov/centers/eros/science/usgs-eros-archive-digital-elevation-shuttle-radar-topography-mission-srtm-1

USGS. (2023c). What are the band designations for the Landsat satellites? United States Geological Survey. https://www.usgs.gov/faqs/what-are-band-designations-landsat-satellites#:~:text=Landsat 1-5 Multispectral Scanner,106 mi by 115 mi)

Vishwakarma, C. A., Thakur, S., Rai, P. K., Kamal, V., & Mukherjee, S. (2016). Changing land trajectories: A case study from india using a remote sensing based approach. *European Journal of Geography,* 7(2), 61–71. https://www.eurogeojournal.eu/index.php/egj/article/view/396

Wallace, C. S. A., Thenkabail, P., Rodriguez, J. R., & Brown, M. K. (2017). Fallow-land Algorithm based on Neighborhood and Temporal Anomalies (FANTA) to map planted versus fallowed croplands using MODIS data to assist in drought studies leading to water and food security assessments. *GIScience & Remote Sensing,* 45(2). https://doi.org/10.1080/15481603.2017.1290913

Wilson, S. A., & Wilson, C. O. (2013). Modelling the impacts of civil war on land use and land cover change within Kono District, Sierra Leone: A socio-geospatial approach. *Geocarto International,* 28(6), 476–501. https://doi.org/10.1080/10106049.2012.724456

Winowiecki, L., Vågen, T. G., & Huising, J. (2015). Effects of land cover on ecosystem services in Tanzania: A spatial assessment of soil organic carbon. *Geoderma,* 263, 274–283. https://doi.org/10.1016/j.geoderma.2015.03.010

Zakhem, B. A., & Hafez, R. (2010). Climatic factors controlling chemical and isotopic characteristics of precipitation in Syria. *Hydrological Processes,* 24(18), 2641–2654. https://doi.org/10.1002/hyp.7646

Zambon, I., Serra, P., Salvia, R., & Salvati, L. (2018). Fallow land, recession and socio-demographic local contexts: Recent dynamics in a Mediterranean urban fringe. *Agriculture (Switzerland),* 8(10). https://doi.org/10.3390/agriculture8100159

https://doi.org/10.48088/ejg.a.you.14.3.020.041